Nucleic Acids Research, 2024, **52**, 4627–4643
https://doi.org/10.1093/nar/gkae087
Advance access publication date: 15 February 2024
RNA and RNA-protein complexes

Ribosomal collision is not a prerequisite for ZNF598-mediated ribosome ubiquitination and disassembly of ribosomal complexes by ASCC

Anna Mišcicka[†], Alexander G. Bulakhov[†], Kazushige Kuroha, Alexandra Zinoviev, Christopher U.T. Hellen and Tatyana V. Pestova[*]

Department of Cell Biology, SUNY Downstate Health Sciences University, Brooklyn, NY, USA

[*]To whom correspondence should be addressed. Tel: +1 718 270 1034; Fax: +1 718 270 2656; Email: tatyana.pestova@downstate.edu
[†]The first two authors should be regarded as Joint First Authors.
Present addresses:
Kazushige Kuroha, Department of Histology and Cell Biology, Yokohama City University School of Medicine, Yokohama 236-0004, Japan.
Alexandra Zinoviev, Eli Lilly and Company, Cambridge, MA 02142, USA.

Abstract

Ribosomal stalling induces the ribosome-associated quality control (RQC) pathway targeting aberrant polypeptides. RQC is initiated by K63-polyubiquitination of ribosomal protein uS10 located at the mRNA entrance of stalled ribosomes by the E3 ubiquitin ligase ZNF598 (Hel2 in yeast). Ubiquitinated ribosomes are dissociated by the ASC-1 complex (ASCC) (RQC-Trigger (RQT) complex in yeast). A cryo-EM structure of the ribosome-bound RQT complex suggested the dissociation mechanism, in which the RNA helicase Slh1 subunit of RQT (ASCC3 in mammals) applies a pulling force on the mRNA, inducing destabilizing conformational changes in the 40S subunit, whereas the collided ribosome acts as a wedge, promoting subunit dissociation. Here, using an *in vitro* reconstitution approach, we found that ribosomal collision is not a strict prerequisite for ribosomal ubiquitination by ZNF598 or for ASCC-mediated ribosome release. Following ubiquitination by ZNF598, ASCC efficiently dissociated all polysomal ribosomes in a stalled queue, monosomes assembled in RRL, *in vitro* reconstituted 80S elongation complexes in pre- and post-translocated states, and 48S initiation complexes, as long as such complexes contained ≥ 30–35 3′-terminal mRNA nt. downstream from the P site and sufficiently long ubiquitin chains. Dissociation of polysomes and monosomes both involved ribosomal splitting, enabling Listerin-mediated ubiquitination of 60S-associated nascent chains.

Graphical abstract

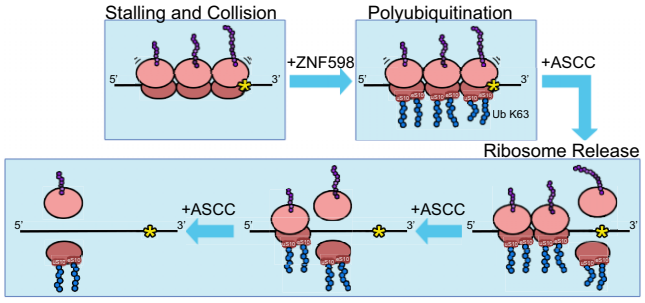

Introduction

To ensure the accuracy of gene expression, eukaryotic cells developed highly conserved mRNA and protein quality control systems that are induced by ribosomal stalling. Thus, the No-Go decay (NGD) surveillance mechanism targets mRNAs on which ribosomal elongation complexes (ECs) are stalled by e.g. stable secondary structures, rare codons, polyA stretches or damaged RNA bases (1–3), whereas corresponding nascent chain (NC) polypeptides arising from interrupted translation undergo degradation by the ribosome-associated quality control (RQC) pathway (4,5). The RQC is initiated by K63-polyubiquitination of specific 40S ribosomal proteins located in the vicinity of the mRNA entrance (uS10 and eS10 in mammals and uS10 in yeast) by the E3 ubiquitin ligase ZNF598 (Hel2 in yeast) (6–11), which triggers dissociation of stalled ribosomes by the ASC-1 (activating signal cointegrator 1) complex (ASCC) (the RQC-Trigger (RQT) complex in yeast) into 40S subunits and NC-tRNA/60S ribosome-nascent chain complexes (60S RNCs) (9,12–14). 60S RNCs associate with NEMF (Rqc2 in yeast), which recruits the E3 ligase Listerin (Ltn1 in yeast) that ubiquitinates NCs (15–17), after which ANKZF1 (Vms1 in yeast) induces specific

Received: December 1, 2023. **Revised:** January 12, 2024. **Editorial Decision:** January 15, 2024. **Accepted:** January 29, 2024

cleavage in the tRNA acceptor arm, releasing proteasome-degradable Ub-NCs linked to three 3′-terminal tRNA nucleotides (18–21).

The first step in RQC is recognition of ribosomal stalling by ZNF598/Hel2. Although the exact ribosomal positions of ZNF598/Hel2 have not been determined, it is thought that their binding is facilitated by direct recognition of the specific interface formed by the 40S subunits of collided ribosomes (8,11,22). Mammalian and yeast disomes have the overall conserved architecture, in which the leading ribosome is stalled in the classical post-translocated state with the P/P site tRNA and the colliding ribosome is locked in the pre-translocated state with P/E and A/P tRNAs (8,11,22,23), with the exception of polysomes stalled on a polyA tract, where a large proportion of the first collided ribosomes were also in post-translocated states due to less rigid arrest of the leading ribosome (24). However, the intersubunit interface and contacts between the colliding ribosomes in mammals and yeast differ significantly (22). Thus, in the main RQC signaling 40S head-to-head contact area, mammalian RACK1 proteins do not interact with each other in contrast to their yeast Asc1 counterparts, and the position of yeast eS10 is rotated away from the leading ribosome compared to mammalian eS10 (11,22). It was suggested that this difference could be responsible for the distinct specificities of ZNF598 and Hel2, i.e. lack of eS10 ubiquitination by Hel2, and that the closer contact between yeast ribosomes could potentially explain the higher stability and smaller hinging movements in the yeast disome (22). Although mammalian ZNF598 additionally polyubiquitinates eS10 (22), the fact that polyubiquitinated uS10 rather than eS10 was detected in ASCC-dissociated 40S subunits led to the suggestion that, like in yeast, ribosomal dissociation in mammals is also triggered by polyubiquitination of uS10 (22). It was also reported that Hel2 mediates polyubiquitination of uS3 following its mono-ubiquitination by Mag2, the yeast homolog of mammalian the E3 ubiquitin ligase RNF10 (25).

K63-polyubiquitination of stalled ribosomes by ZNF598/Hel2 is followed by their disassembly by ASCC/RQT complexes. The yeast RQT complex comprises the Ski2-like tandem-helicase cassette RNA helicase Slh1, the ubiquitin-binding CUE domain containing protein Cue3 and the zinc-finger containing protein Rqt4 (9,12). The mammalian ASCC contains four subunits, three of which are homologous to the subunits of the yeast RQT: ASCC3 (a homologue of Slh1), ASCC2 (a homologue of Cue3) and TRIP4/Asc-1 (a homologue of Rqt4) (26). The fourth subunit, ASCC1, is essential for the nuclear function of ASCC in DNA repair (27) but is dispensable for dissociation of stalled ribosomes (13,28). The ATP-dependent helicase activity of Slh1/ASCC3 (29,30) is essential for ribosomal splitting (9,13,14,23,31). Although it was previously suggested that ASCC2 ubiquitin-binding activity (32,33) is dispensable for the ASCC function (14), more recent studies indicate that it is also required for ASCC-mediated ribosomal splitting (13,22). Interestingly, in yeast, both the CUE domain of Cue3 and the N-terminal domain of Rqt4 bind independently to the K63-linked Ub chains to promote recruitment of the RQT complex to ubiquitinated ribosomes (34). The overhanging 3′-terminal region of mRNA was shown to be also essential for the RQT-mediated ribosomal splitting (23). Moreover, efficient ribosomal splitting by RQT required at least one collided neighboring ribosome (23).

A recent cryo-EM structure of the ribosome-bound RQT complex shed light on the molecular mechanism of ribosomal splitting (23). The RQT complex was located on the 40S subunit of the leading ribosome in proximity to the mRNA entry channel and uS10. On the collided ribosome, the RQT binding site was shielded by the leading ribosome, which is in line with the observed sequential nature of polysomal disassembly (14,31). Slh1 adopted the bi-lobed arch-like architecture formed by two helicase cassettes, which was stabilized by Cue3 and Rqt4 positioned between the cassettes. The N-terminal cassette resided at the mRNA entrance, stretching from helix 16 along eS10, uS3 and uS10, whereas the C-terminal cassette interacted with Asc1. Strikingly, the RQT complex associated with 80S ribosomes in two different conformations: the pre-splitting classical post-translocation state with tRNA in the P/P site, and another state, in which the 40S head was swiveled by 20 degrees relative to the 40S body resulting in the 80S conformation similar to that of a translocation intermediate with tRNA in the chimeric pe/E hybrid state (35). Since the transition from the pre-splitting post-translocation to head-swiveled states could be achieved by applying force to the mRNA in the direction opposite to mRNA translocation, the pulling mechanism of ribosomal splitting was proposed. In this mechanism, Slh1 would apply a pulling force on the mRNA, inducing destabilizing conformational changes in the 40S subunit, whereas the collided ribosome would act as a wedge, enabling subunit dissociation. This mechanism poses a question of which Slh1 helicase cassette is executing mRNA pulling. Although no clear mRNA density was identified in either Slh1 cassette, the relative positions of the cassettes with respect to the mRNA path at the mRNA entrance led to the suggestion that the C-terminal cassette is more likely to bind mRNA and extract it from the 40S subunit.

It was recently suggested that in addition to its role in RQC, mammalian ASCC stimulates initiation by scanning ribosomal complexes on a subset of cellular mRNAs containing stable secondary structures in their 5′UTRs (36). The reported activity of ASCC in initiation is difficult to reconcile with the pulling mechanism proposed for the RQT-mediated ribosomal splitting. However, it is worth noting that according to the structure of the ribosome-bound RQT complex, direct threading of mRNA at the mRNA entrance into the helicase core of the N-terminal cassette of Shl1 might result in 5′-3′ feeding of mRNA into the 40S subunit rather than its extraction (23).

Here, we applied an *in vitro* reconstitution approach to investigate the requirements for ASCC-mediated ribosomal splitting. Strikingly, we found that ribosomal collision is not a strict prerequisite for ribosomal ubiquitination by ZNF598 or for ASCC-mediated ribosome release, and ASCC efficiently dissociated all polysomal ribosomes in a stalled queue, including the last one, monosomes and also 48S initiation complexes as long as all these complexes were polyubiquitinated by ZNF598 and contained sufficiently long overhanging 3′-terminal mRNA regions.

Materials and methods

Elongation activity of ribosomal complexes stalled on the polyA tract

Sucrose density gradient (SDG) purified [^{35}S]-labeled monosomes or disomes assembled on β-VHP-A39 mRNA were

incubated for 40 min at 32°C with the indicated combinations of 80 nM eEF1H, 80 nM eEF2, 500 nM Lys-tRNA^{Lys}, native Σaa-tRNA (880 nM calculated on the basis of Met-tRNA$_i^{Met}$) and 100 nM eRF1•eRF3•GTP in 20 μl buffer A (20 mM Tris pH 7.5, 100 mM KCl, 2 mM DTT, 0.25 mM spermidine) supplemented with 1 mM ATP, 1 mM GTP, 12 mM creatine phosphate, 2 U/μl RiboLock RNase inhibitor and MgAc to achieve the indicated free [Mg^{2+}]. When indicated, after translation, reaction mixtures were treated with 60 μg/ml RNaseA for 10 min at 32°C. Reactions were stopped by adding loading buffer. Translation products were resolved by 4–12% NuPAGE Bis-Tris electrophoresis and visualized by Phosphoimager. All experiments were repeated two to three times.

In vitro ubiquitination of individual 40S subunits, vacant 80S ribosomes and polysomes by ZNF598 and RNF10, and substrate-independent synthesis of poly-ub chains by ZNF598

For ubiquitination by ZNF598, 125 nM of 40S subunits or vacant 80S ribosomes or 75 nM of β-VHP-A39 polysomes were incubated for 30 min at 37°C with 3 μM *wt* or indicated mutant Ub, 120 nM Ube1, 1.33 μM indicated Ube2 enzymes (R&D Systems, Minneapolis MN) and 300 nM ZNF598 in 40 μl buffer A supplemented with 2 mM ATP and $MgCl_2$ to achieve 2 mM free [Mg^{2+}]. To assay the specificity of Ub linkage, we employed K63 only, K48 only and K63R Ub mutants. In the first two mutants, all other six lysines except K63 or K48 were replaced by arginine, whereas in the third mutant, only K63 was replaced by arginine. For ubiquitination of SERBP1/eEF2-bound ribosomes, vacant 80S ribosomes were first preincubated with 400 nM SERBP1 with or without 400 nM eEF2 for 10 min in 37°C, followed by ZNF598-mediated ubiquitination as described above. To analyze substrate-independent poly-Ub synthesis by ZNF598, reaction conditions were as described above, except that 40S subunits or 80S ribosomes were omitted from reaction mixtures.

For ubiquitination with RNF10 and ZNF598, 62.5 nM vacant 80S ribosomes were preincubated with or without 190 nM EDF1 for 10 min at 37°C in 40 μl buffer A supplemented with 2 mM ATP and $MgCl_2$ to achieve 2 mM free [Mg^{2+}]. 4.1 μM *wt* Ub, 120 nM Ube1, 1.33 μM Ube2D3 and 350 nM ZNF598 and/or RNF10 were then added to reaction mixtures, and incubation continued for another 20 min.

In all cases, reactions were terminated by addition of loading buffer. Ubiquitination products were resolved by 4–12% NuPAGE Bis-Tris electrophoresis and visualized by western blotting. All experiments were repeated at least three times.

Analysis of ASCC-mediated release of ribosomal complexes by toeprinting

To examine the activity of ASCC, 20–30 nM of indicated SDG-purified ribosomal complexes (RRL-assembled polysomes/monosomes or *in vitro* reconstituted 80S or 48S complexes) were first ubiquitinated for 30 min at 37°C with 300 nM ZNF598, 120 nM Ube1, 1.2 μM Ube2D3 and 2.75 μM *wt* or indicated mutant Ub in 80–120 μl buffer A supplemented with 1 mM ATP, 1 mM GTP, 12 mM creatine phosphate, 2 U/μl RiboLock RNase inhibitor, 30 μg/ml Creatine Kinase and $MgCl_2$ to achieve 2 mM free [Mg^{2+}]. Where indicated, 300 nM of RNF10 was added with ZNF598. Reaction mixtures were then supplemented with 100 nM ASCC (estimated by the amount of ASCC3), and incubation continued for 10 min except when ASCC was included at the beginning with ZNF598. Where indicated, reaction mixtures also contained combinations of 300 nM eEF2, 200 nM eRF1, 200 nM eRF3, 200 nM eRF1(AGQ), 100 nM ABCE1 and 100 nM Ligatin. Resulting ribosomal complexes were analyzed by primer extension (37) using AMV reverse transcriptase (RT) (Promega) and [^{32}P]-labeled primers. cDNA products were resolved on 6% polyacrylamide sequencing gels and visualized by Phosphoimager. All experiments were repeated at least three times.

Time courses of ASCC-mediated release of monosomes and polysomes assayed by toe-printing

20 nM of indicated ZNF598-polyubiquitinated SDG-purified ribosomal complexes were incubated for the indicated times at 37°C with 200 nM ASCC (estimated by the amount of ASCC3) in 100 μl buffer A supplemented with 1 mM ATP, 1 mM GTP, 12 mM creatine phosphate, 2 U/μl RiboLock RNase inhibitor and $MgCl_2$ to achieve 2 mM free [Mg^{2+}]. 300 nM eEF2 was included where indicated. At indicated timepoints, the reaction was stopped by elevation of free [Mg^{2+}] to 20 mM and placed on ice. For timepoint 0′, free [Mg^{2+}] was increased to 20 mM before adding ASCC and the sample was incubated at 37°C for 5 min and placed on ice when the final time point was collected. The resulting ribosomal complexes were analyzed by toe-printing (37). All experiments were repeated three times.

Analysis of Listerin-mediated ubiquitination of NCs following ASCC-induced ribosome release

20–30 nM of the indicated RRL-assembled SDG-purified ribosomal complexes were incubated for 30 min at 37°C with indicated combinations of 300 nM ZNF598, 120 nM Ube1, 1.2 μM Ube2D3, 2.75 μM *wt* or mutant Ub, 100 nM NEMF, 100 nM Listerin and 100 nM ASCC in 40 μl buffer A supplemented with 2 mM ATP, 2 U/μl RiboLock RNase inhibitor and $MgCl_2$ to achieve 2 mM free [Mg^{2+}]. In all cases, reactions were terminated by adding loading buffer. Ubiquitination products were resolved by 4–12% NuPAGE Bis-Tris electrophoresis and visualized by Phosphoimager. All experiments were repeated at least three times.

Analysis of ASCC-mediated ribosome release by SDG centrifugation

SDG-purified pre-TCs reconstituted *in vitro* on [^{32}P]-labeled β-MLLFF-Stop mRNAs containing 17nt- or 27nt-long 3′UTRs were ubiquitinated by ZNF598 and then incubated with ASCC in a 120 μl reaction volume as described above. After incubation, reaction mixtures were subjected to centrifugation in a Beckman SW55Ti rotor at 53 000 rpm for 80 min at 4°C in 10–30% linear SDGs prepared in buffer B (20 mM Tris pH 7.5, 100 mM KCl, 1.5 mM $MgCl_2$, 2 mM DTT and 0.25 mM spermidine). After fractionation, [^{32}P]-labeled β-MLLFF-Stop mRNA was quantified by liquid scintillation counting. All experiments were repeated at least three times.

Analysis of ASCC-mediated dissociation of preubiquitinated ribosomal complexes

SDG-purified poly- or oligoubiquitinated ribosomal complexes were incubated with 100 nM ASCC with/without 300 nM of ZNF598 in 40 μl of buffer A supplemented with 1 mM ATP, 1 mM GTP, 12 mM creatine phosphate, 2 U/μl RiboLock RNase inhibitor, 30 μg/ml Creatine Kinase and $MgCl_2$ to achieve 2 mM free [Mg^{2+}] for 30 min. Ribosomal complexes were then analyzed by toe-printing (37). All experiments were repeated at least three times.

The influence of ASCC and the Ski complex on 48S initiation complexes

To assay the influence of ASCC on 48S complex formation, 40 nM of (AUG at -6)-STEM mRNA was incubated in 40 μl of buffer A supplemented with 1 mM ATP, 1 mM GTP, 12 mM creatine phosphate, 2 U/μl RiboLock RNase inhibitor, 30 μg/ml Creatine Kinase and $MgCl_2$ to achieve 2 mM free [Mg^{2+}] with indicated combinations of 75 nM 40S, 150 nM Met-tRNA$_i^{Met}$, 200 nM eIF2, 140 nM eIF3, 150 nM eIF4A, 600 nM eIF4A, 25 nM eIF4G$_{736\text{-}1600}$, 500 nM eIF1 and 375 nM eIF1A, 300 nM ZNF598, 120 nM Ube1, 1.2 μM Ube2D3 and 2.75 μM *wt* Ub and 150 nM DHX29 for 15 min at 37°C. Where indicated, 150 nM ASCC was added with other components or after 15 min, in which case incubation continued for an additional 15 min. Ribosomal complexes were then analyzed by toe-printing (37).

To assay the influence of ASCC and the Ski complex on preassembled 48S complexes, 20 nM SDG purified 48S complexes *in vitro* reconstituted β-MF-Stop mRNA were incubated with 100 nM Ski complex or with 300 nM ZNF598, 120 nM Ube1, 1.2 μM Ube2D3 and 2.75 μM *wt* Ub and 150 nM ASCC for 30 min at 37°C in 40 μl buffer A supplemented with 1 mM ATP, 1 mM GTP, 2 U/μl RiboLock RNase inhibitor and $MgCl_2$ to achieve 2 mM free [Mg^{2+}]. Ribosomal complexes were then analyzed by toe-printing (37).

All experiments were repeated at least three times.

The effect of RNF10 on ribosomal complexes assayed by toe-printing

The effect of RNF10 was analyzed using *in vitro* reconstituted 80S ICs and pre- or post-translocated collided ribosomes formed in RRL. 20 nM SDG-purified 80S ICs assembled on β-MF-Stop mRNA were incubated for 30 min at 37°C with the indicated combination of 300 nM RNF10, 120 nM Ube1, 1.2 μM Ube2D3 and 2.75 μM *wt* Ub in 80 μl buffer A supplemented with 1 mM ATP, 1 mM GTP, 12 mM creatine phosphate, 2 U/μl RiboLock RNase inhibitor, 30 μg/ml Creatine Kinase and $MgCl_2$ to achieve 2 mM free [Mg^{2+}]. 20 nM SDG-purified disomes stalled on the stop codon of β-VHP-Stop mRNA were incubated with 200 nM eRF1, 200 nM eRF3, 100 nM ABCE1 and 100 nM Ligatin with/without 300 nM eEF2 for 15 min at 37°C in 80 μl buffer A supplemented with 1 mM ATP, 1 mM GTP, 12 mM creatine phosphate, 2 U/μl RiboLock RNase inhibitor, 30 μg/ml Creatine Kinase and $MgCl_2$ to achieve 2 mM free [Mg^{2+}]. Reaction mixtures were then supplemented with 300 nM RNF10, 120 nM Ube1, 1.2 μM Ube2D3 and 2.75 μM *wt* Ub and incubated for another 30 min. Ribosomal complexes were then analyzed by toe-printing (37). All experiments were repeated two to three times.

Results

Ubiquitination activity of ZNF598

Before investigating ribosome release by ASCC, we characterized the ubiquitination activity of purified recombinant FLAG-tagged ZNF598 (Figure 1A). ZNF598 was equally active on individual 40S subunits and vacant 80S ribosomes, and as reported (6,7,9,10), ubiquitinated eS10 and uS10 and exhibited specificity for Ube2D family E2s (shown for 40S subunits in Figure 1B). Based on the relative availability of different Ube2Ds in our laboratory at that time, Ube2D3 was chosen for all subsequent experiments. In line with the K63-specificity of its yeast homologue Hel2 (25,34,38) and consistent with a more recent report on ZNF598 (22), it promoted polyubiquitination of eS10 and uS10 with *wt* and K63 single-Lys Ub (Figure 1C). We note that throughout all experiments, antibodies against uS10 recognized the highly polyubiquinated protein less efficiently than its non- and oligoubiquitinated forms.

With K63R Ub, eS10 was di- and tri-ubiquitinated, whereas uS10 was mostly di-ubiquitinated, with small amounts being tri- and tetra-ubiquitinated (Figure 1C). Since both proteins can be ubiquitinated at two closely situated sites: K138 and K139 in eS10, and K4 and K8 in uS10 (7,10), the appearance of tri- and tetra-ubiquitinated uS10 and eS10 suggested that ZNF598 promoted formation of short Ub chains with non-K63 linkage. To confirm this, 40S subunits were ubiquitinated with K48 single-Lys Ub, and ubiquitination was monitored by western blotting using antibodies specific either for ribosomal proteins or for the K48 linkage. Di-ubiquitinated uS10 was detected only by antibodies against uS10, indicating concurrent mono-ubiquitination at K4 and K8 (Figure 1D, upper panel). However, tri- and tetra-ubiquitinated uS10 was detected by both antibodies, showing that ZNF598 could assemble di-Ub chains with non-K63 linkage (Figure 1D, upper panel). Di-ubiquitinated eS10 was also detected by both antibodies (Figure 1D, lower panel), but it migrated very close to tetra-ubiquitinated uS10, so we could not determine with certainty whether it had been mono-ubiquitinated at two sites or contained di-Ub chains. However, tri-ubiquitinated eS10 was unambiguously detected by both antibodies, indicating that on this ribosomal protein, ZNF598 could also assemble at least di-Ub chains with non-K63 linkage. Strikingly, in the absence of a substrate, ZNF598 efficiently synthesized poly-Ub chains with K63 linkage (Figure 1E), which suggests that it contains a binding site for the acceptor ubiquitin, orienting it such that K63 is positioned to attack the E2∼Ub conjugate.

Although ZNF598 did not strictly require ribosomal collision and efficiently ubiquitinated individual 40S subunits and vacant 80S ribosomes in our experiments, we noticed that in rabbit reticulocyte lysate (RRL), ubiquitination of 80S ribosomes by ZNF598 was poor. Although this might be due to engagement of ZNF598 with other potential targets or high deubiquitinase activity in the cell-free extract, the association of non-programmed 80S ribosomes from RRL (as well as in human peripheral blood mononuclear cells, and in *Drosophila melanogaster* embryonic extracts) with SERPINE1 mRNA binding protein 1 (SERBP1) and eEF2 (39–41) could also influence ubiquitination. The ribosome preservation factor SERBP1 binds to the head of the 40S subunit and then enters the mRNA-binding channel and follows the mRNA-binding path until the A site where it interacts with domain IV of eEF2 (39,41). Indeed, preincubation of

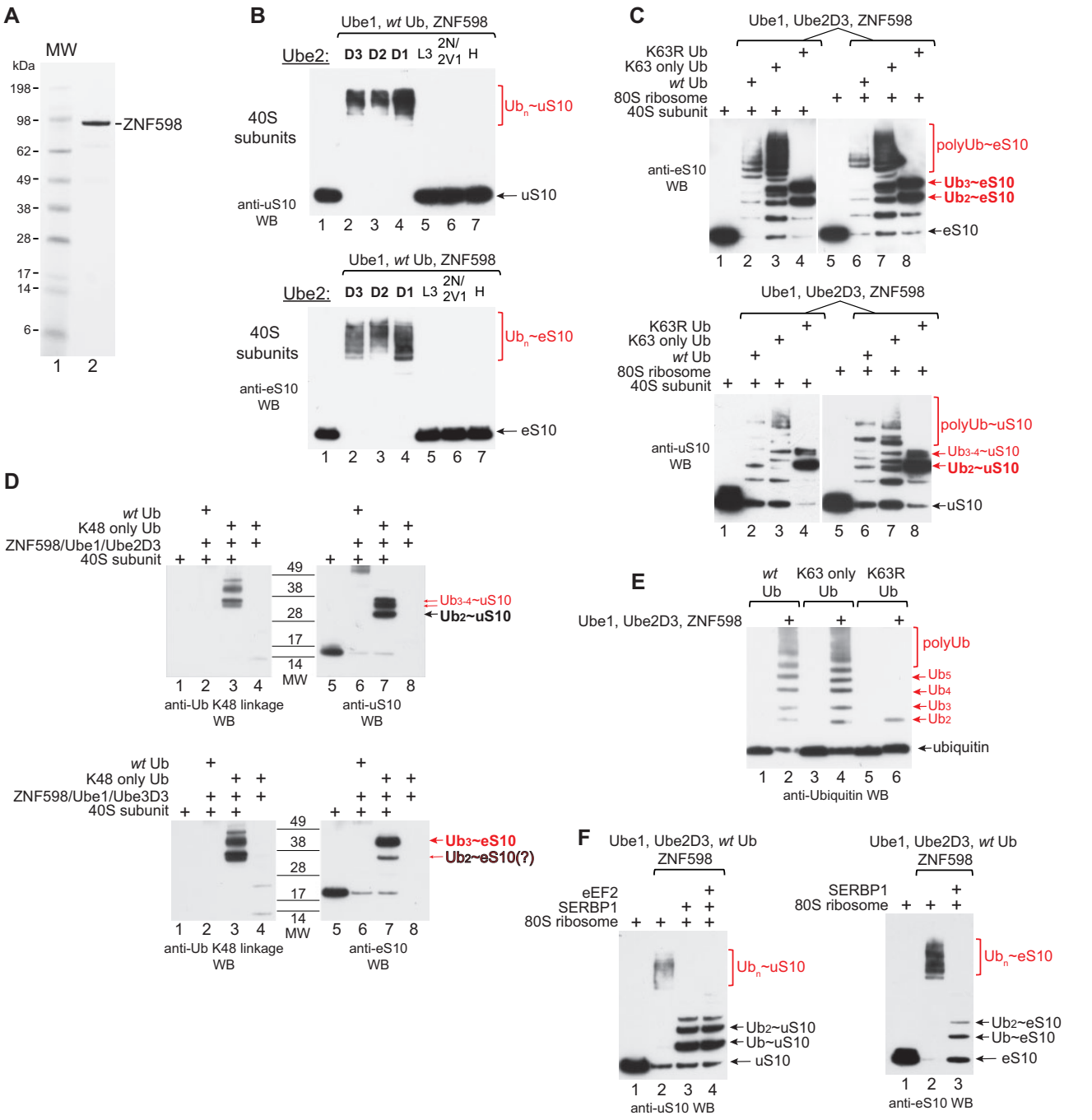

Figure 1. Ribosomal ubiquitination by ZNF598. (**A**) Purified ZNF598, analyzed by SDS-PAGE and SimplyBlue staining. (**B**) Ubiquitination of uS10 and eS10 in 40S subunits by ZNF598 with Ube1, *wt* Ub and Ube2 ubiquitin-conjugating enzymes as indicated, assayed by western blotting using antibodies against uS10 or eS10. (**C**) Ubiquitination of eS10 and uS10 in 40S subunits and vacant 80S ribosomes by ZNF598 with Ube1, Ube2D3, and *wt*, K63 only or K63R Ub, as indicated, assayed by western blotting using antibodies against eS10 or uS10. (**D**) Ubiquitination of uS10 and eS10 in 40S subunits by ZNF598 with Ube1, Ube2D3 and *wt* or K48 only Ub, assayed by western blotting using antibodies against K48 linkage (lanes 1–4) or ribosomal proteins (lanes 5–8). (**E**) Synthesis of poly-Ub chains by ZNF598 with Ube1, Ube2D3 and *wt*, K63 only or K63R Ub, as indicated, assayed by western blotting using anti-Ub antibodies. (**F**) Influence of SERBP1 and eEF2 on ubiquitination of uS10 and eS10 in 40S subunits and 80S ribosomes by ZNF598 with Ube1, Ube2D3 and *wt* Ub, assayed by western blotting using antibodies against uS10 or eS10.

purified vacant 80S ribosomes with SERBP1 with or without eEF2 strongly reduced ubiquitination of uS10 and eS10 by ZNF598 (Figure 1F).

Preparation and characterization of polysomes

To investigate the activity of ASCC, we decided to employ polysomes stalled at a stop codon, which mimic stalling on a rare codon, and on a polyA tract, a natural staller that triggers RQC in mammals (7). The choice of these polysomes was based on differences in their structures: on the former, the first collided ribosome next to the stalled ribosome is in the pre-translocated state, whereas on the latter, this collided ribosome is in the post-translocated state (24,31).

Polysomes stalled at a stop codon were assembled on β-VHP-Stop mRNA (18,42) comprising the β-globin 5′UTR followed by the coding region for the short structured villin headpiece (VHP) and an unstructured region of Sec61β, a UAG stop codon, and a 94nt.-long 3′UTR (Figure 2A; (18)). Polysomes were obtained by translating β-VHP-Stop mRNA in RRL in the presence of eRF1^{AGQ} mutant (with a G183A substitution in the essential GGQ motif), which can bind to pre-TCs but cannot trigger peptide release and therefore arrests ribosomal complexes at the pre-termination stage. Subsequent SDG centrifugation dissociated eRF1^{AGQ} (40), yielding factor-free monosomes and polysomes (Figure 2B, upper left panel) with NC-tRNAs containing NCs of the expected molecular weight (Figure 2B, lower left panel), and toe-prints consistent with arrest of the leading ribosome at the stop codon (Figure 2B, right panel). Interestingly, toe-prints corresponding to monosomes and polysomes showed distinct relative intensities of individual bands (Figure 2B, right panel, compare lane 3 with lanes 1–2), which could indicate subtle structural differences between individual post-translocated 80S ribosomes and the leading ribosomes in collided queues.

Next, we investigated translation in RRL of mRNAs containing polyA sequences of various lengths inserted at the 3′-terminal end of the coding region of β-VHP-Stop mRNA and followed by an in-frame UAG stop codon and a 42nt-long 3′-UTR with two additional out-of-frame stop codons, UAG(+1) and UGA(−1) (Figure 2C, upper panel). mRNAs containing up to 5 consecutive AAA Lys codons yielded completed products that were released at the stop codon, whereas extension of the polyA tract up to 39 nucleotides resulted in progressive stalling, and accumulation of NC-tRNAs (Figure 2C, lower left panel). Whereas 39 consecutive adenines (corresponding to 13 AAA Lys codons) induced strong stalling, mRNA containing 13 consecutive AAG Lys codons yielded a completed released polypeptide (Figure 2C, bottom right panel). The length of polyA required for stalling and the observation that stalling was dependent on the mRNA sequence rather than the encoded oligopeptide are consistent with a prior report (43).

Because 13 consecutive AAA Lys codons caused efficient stalling, polysomes arrested on the polyA tract were formed by translating in RRL of β-VHP-A39 mRNA. After translation, polysomes were purified by SDG centrifugation (Figure 2D, top left panel). In monosomes and polysomes, the leading ribosome yielded a wide set of toe-prints with the most intense occurring at AAAA$_{18\text{-}21}$ (Figure 2D, right panel), which correspond to stalling at the second or third AAA codon in the P site. Weaker toe-prints downstream of AAAA$_{18\text{-}21}$ indicated that some ribosomes penetrated further into the polyA tract. Accordingly, in addition to the NCs corresponding to the main stall, NCs of higher molecular weight were observed (Figure 2D, bottom left panel).

Consistent with the detrimental effect of high [Mg^{2+}] on initiation, elevation of [Mg^{2+}] in RRL above the optimum progressively reduced translation of β-VHP-A39 mRNA, but at the same time it stimulated readthrough of polyA, resulting in accumulation of completed released NCs (Figure 2E). At elevated [Mg^{2+}], purified monosomes were also able to resume translation of polyA upon addition of eEFs and Lys-tRNA^{Lys} (Figure 2F). In disomes, the leading ribosome, but not the collided one, elongated in the presence of eEFs and Lys-tRNA^{Lys} (Figure 2G, lanes 1 and 3), but eRFs did not release NCs from all slower migrating NC-tRNAs (Figure 2G, lane 4), indicating that a proportion of leading ribosomes underwent frameshifting and did not contain the stop codon in the A site. In the presence of total aa-tRNAs, both leading and collided ribosomes were able to elongate, but in addition to slower migrating NC-tRNAs containing the Lys stretch, we observed even more slowly migrating NC-tRNAs corresponding to NCs that extended into the 3′-UTR, which we concluded had reached the UAG (−1 frame) codon because they could be released by eRFs (Figure 2G, lanes 5–6). Thus, in polysomes stalled on the polyA tract, the P site of leading ribosomes was mostly occupied by the second or third Lys codon. However, a proportion of ribosomes penetrated further into the polyA tract and moreover, consistent with previous reports (e.g. (44), some leading ribosomes also underwent frameshifting. Such a relaxed arrest of the leading ribosomes, which could allow the collided ribosome to undergo translocation, was proposed to be the reason for a large proportion of yeast disomes stalled on a polyA tract adopting a post-post translocated state (24).

ASCC-mediated ribosome release in polysomes and monosomes

ASCC was purified from Expi293 cells transfected simultaneously with expression vectors for all four FLAG-tagged subunits. During anti-FLAG M2 affinity chromatography, partial complexes and individual subunits had the opportunity to associate, and subsequent FPLC on MonoS yielded fractions containing the complete ASC-1 complex (Figure 3A). Before investigating the activity of ASCC, we examined ubiquitination by ZNF598 of trisomes formed on β-VHP-Stop and β-VHP-A39 mRNAs (shown for the latter in Figure 3B). For eS10, complete polyubiquitination was observed with *wt* and K63 single-Lys Ub, and di- or tri-ubiquitination with K63R Ub (Figure 3B, left panel). In the case of uS10, ∼90% of the protein was polyubiquitinated with *wt* and K63 single-Lys Ub (again, note that antibodies against uS10 recognized the polyubiquinated protein less efficiently), whereas with K63R Ub, ZNF598 attached 1–4 ubiquitins (Figure 3B, right panel). Complete polyubiquitination of eS10 and ∼90% polyubiquitination of uS10 with *wt* Ub indicated that ZNF598 ubiquitinated all ribosomes irrespective of their position in the collided queue. Ubiquitination with K63R Ub revealed that a substantial proportion of eS10 and uS10 were tri-ubiquitinated and therefore contained di-Ub chains with non-K63 linkage.

To observe sequential ribosome release, polysomal disassembly was assayed by toe-printing. For dissociation of polysomes stalled on polyA, SDG-purified trisomes were ubiquitinated for 30 min by ZNF598 with *wt*, K63 single-Lys or K63R Ub, after which ASCC was added, and incubation

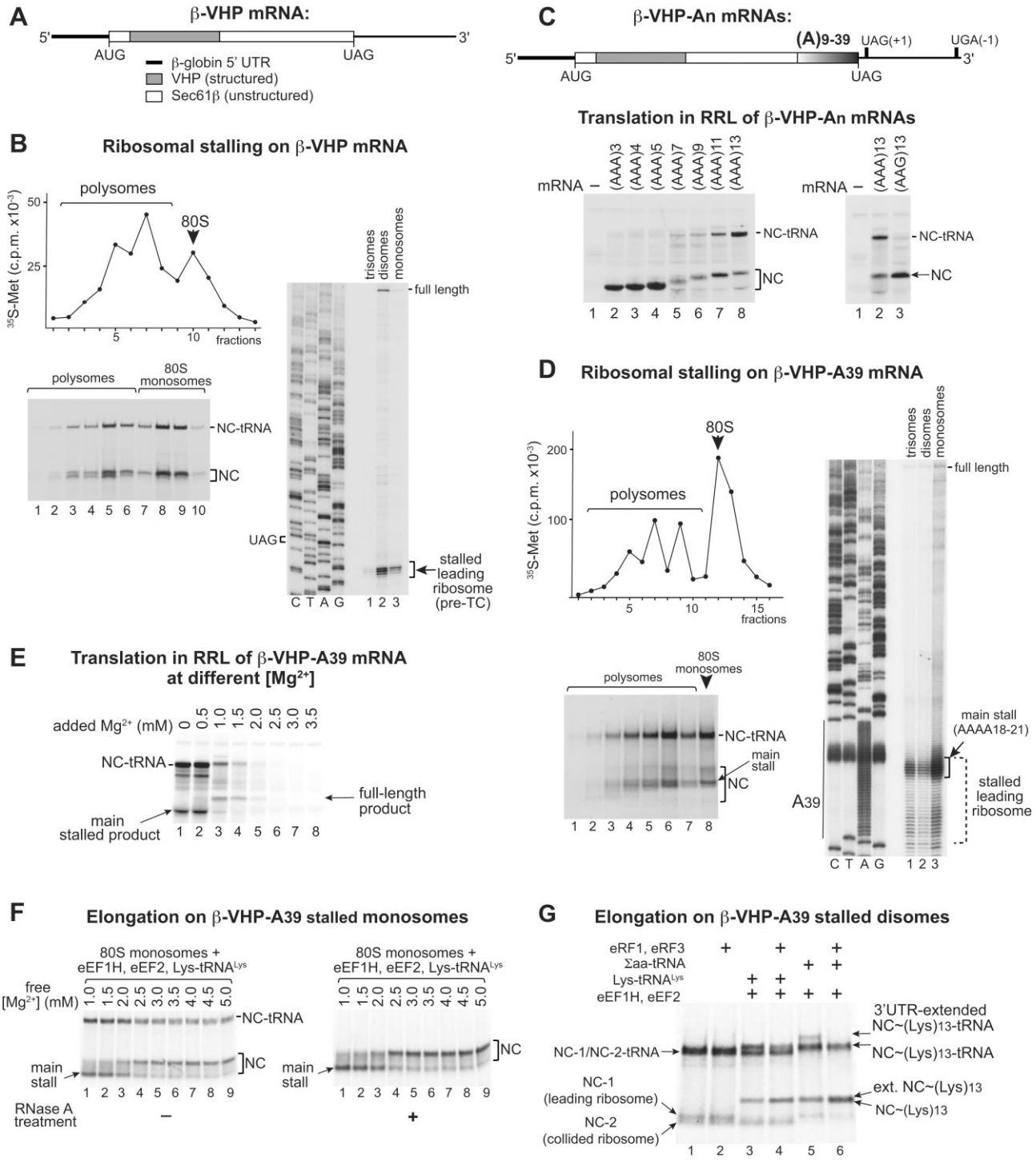

Figure 2. Induction of mammalian ribosomal stalling at the stop codon and at polyA tracts located in the coding region. (**A**) Structural diagram of β-VHP mRNA. (**B**) Ribosomal stalling induced at the stop codon of β-VHP mRNA in RRL by eRF1^{AGQ}, assayed by SDG centrifugation (top left panel), SDS-PAGE to resolve nascent chains (NC) and NC-linked tRNAs (NC-tRNAs) (bottom left panel), and by toe-printing to determine the position of the leading ribosome (right panel). (**C**) Structural diagram of β-VHP-An mRNAs (upper panel). Ribosomal stalling on β-VHP-An mRNAs in RRL as a function of the length of the $(AAA)_n$ and $(AAG)_n$ sequences, assayed by SDS-PAGE to resolve NCs and NC-tRNAs (bottom panels). (**D**) Ribosomal stalling on β-VHP-A39 mRNA in RRL, assayed by SDG centrifugation (top left panel), by SDS-PAGE to resolve NCs and NC-tRNAs (bottom left panel), and by toe-printing to determine the position of the leading ribosome (right panel). (**E**) [Mg^{2+}]-dependence of readthrough in RRL of the A39 sequence in β-VHP-A39 mRNA, assayed by SDS-PAGE. (**F**) [Mg^{2+}]-dependence of readthrough of the A39 sequence by SDG-purified monosomes stalled on β-VHP-A39 mRNA in the presence of eEF1H, eEF2 and Lys-tRNA^{Lys}, with/without subsequent RNase A treatment, assayed by SDS-PAGE. (**G**) Fidelity of elongation through A39 by SDG-purified disomes stalled on β-VHP-A39 mRNA in the presence of eEF1H, eEF2, Lys-tRNA^{Lys} and Σ-aa-tRNA, as indicated, assayed by SDS-PAGE. Frame-shifting was inferred by the ability of ribosomes to translate the 3′-UTR and the sensitivity of NC-tRNAs to eRF1/eRF3-mediated NC release.

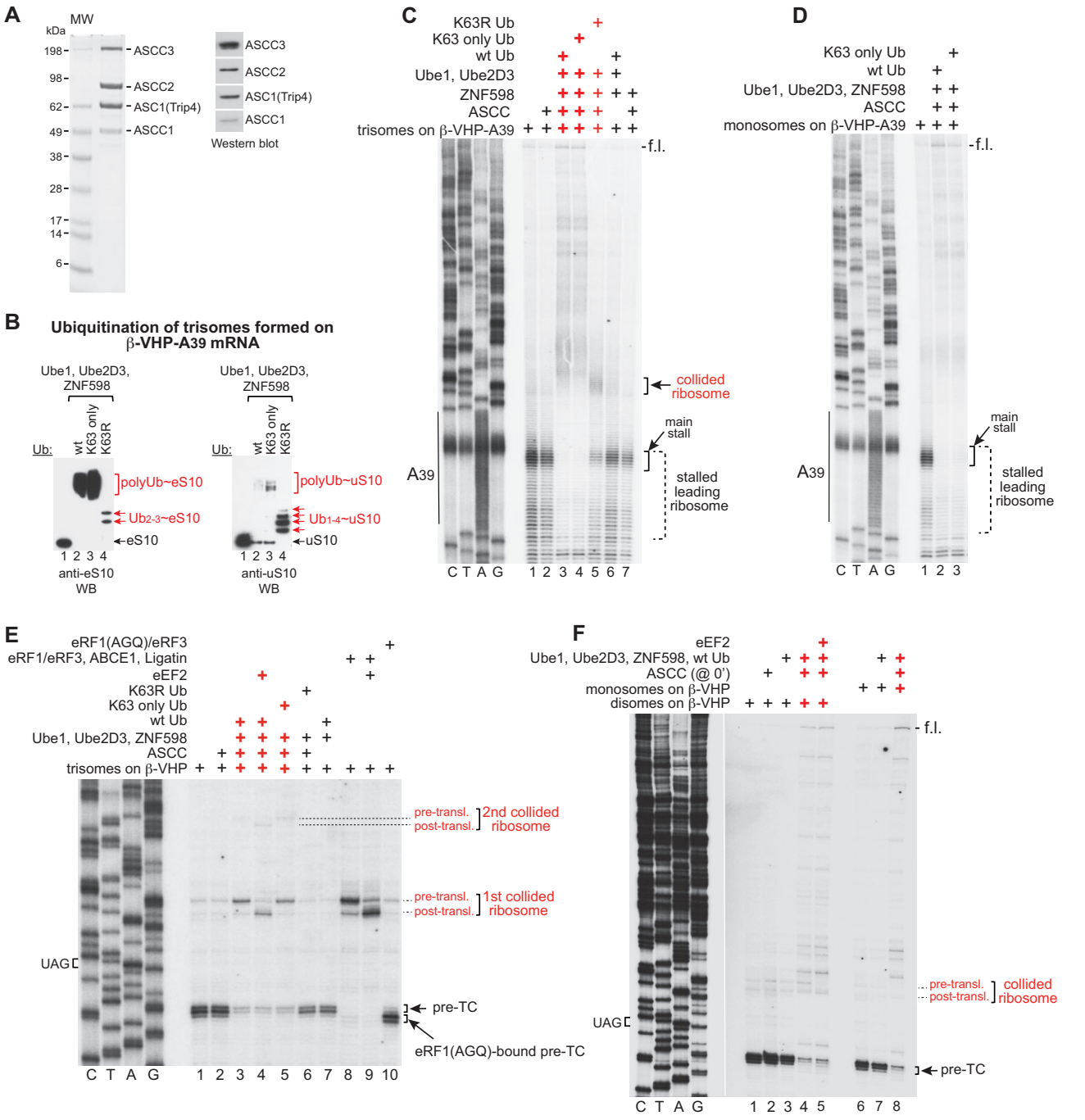

Figure 3. ASCC-mediated dissociation of polysomes stalled on the polyA tract and at the stop codon. (**A**) Purified ASCC, analyzed by SDS-PAGE and SimplyBlue staining or by western blotting using specific antibodies against individual subunits. (**B**) Ubiquitination of eS10 and uS10 in SDG-purified trisomes formed on β-VHP-A39 mRNA by ZNF598 with *wt*, K63 only or K63R Ub, assayed by western blotting. (C, D) ASCC-mediated dissociation of SDG-purified (**C**) trisomes and (**D**) monosomes stalled in RRL on β-VHP-A39 mRNA depending on their ubiquitination by ZNF598 with *wt*, K63 only or K63R Ub, assayed by toe-printing. (E, F) ASCC-mediated dissociation of SDG-purified (**E**) trisomes and (**F**) disomes and monosomes stalled in RRL at the stop codon of β-VHP mRNA depending on their ubiquitination by ZNF598 with *wt*, K63 only or K63R Ub, in the presence/absence of eEF2, assayed by toe-printing. Separation of two parts of the gel in panel F by the white line indicates that the juxtaposed parts were from the same gel but with different exposures.

continued for 10 more min. Dissociation was arrested by the elevation of [Mg^{2+}] that was also required for reverse transcription. When ubiquitination was done with *wt* or K63 single-Lys Ub, ASCC released the leading and both collided ribosomes, yielding full-length mRNA (Figure 3C, lanes 3–4). Surprisingly, when ubiquitination was done with K63R Ub, ASCC was still able to release ∼50% of leading ribosomes exposing the first collided ones which also showed a wide set of toe-prints ∼30 nucleotides upstream of the main stall (Figure 3C, lane 5). This indicates that ASCC could dissociate leading ribosomes with eS10/uS10 tagged with di-Ub chains with non-K63 linkage. ZNF598-mediated ubiquitination alone did not affect the integrity of polysomes, and no release occurred in reaction mixtures containing ASCC and ZNF598 but lacking Ub/E1/E2 (Figure 3C, lanes 6–7). ASCC also efficiently dissociated K63-ubiquitinated stalled monosomes (Figure 3D, lanes 2–3).

In contrast to wide toe-prints exhibited by polysomes stalled on the polyA tract, polysomes stalled on the stop codon showed discrete toe-prints (Figure 2B) which would allow the unambiguous determination of the state of the collided ribosomes. The pre-translocated state of the first collided ribosome was verified by recycling of the leading ribosome by eRFs/ABCE1/Ligatin in the presence/absence of eEF2 (Figure 3E, compare lanes 8 and 9), whereas the absence of $eRF1^{AGQ}$ on the leading ribosome was confirmed by the appearance of the characteristic + 2nt toe-print shift after incubation of trisomes with $eRF1^{AGQ}$/eRF3 ((45); Figure 3E, lane 10). Complete recycling and the + 2nt toe-print shift of the leading ribosomes also suggested a lack of a + 1nt frameshift. 10-min-long incubation of K63-ubiquitinated trisomes with ASCC released the leading ribosome and exposed toe-prints corresponding to the first and the second collided ribosomes with ∼30 nucleotides between toe-prints of all neighboring ribosomes (Figure 3E, lanes 3 and 5). Addition of eEF2 resulted in a characteristic forward shift of toe-prints of both collided ribosomes indicating that in polysomes they were in the pre-translocated state, but it did not affect the efficiency of ribosome release (Figure 3E, lanes 3–5). Thus, dissociation of polysomes stalled at the stop codon seemed somewhat slower than of those stalled on polyA, and no substantial release was observed when ubiquitination was done with K63R Ub (Figure 3E, lane 6). Addition of ASCC at the very beginning of the reaction together with ZNF598 extended the dissociation time and resulted in nearly complete ribosome release and formation of full-length cDNA, irrespective of the presence of eEF2 (Figure 3F, lanes 4 and 5). As in the case of monosomes stalled on the polyA tract, ASCC induced efficient dissociation of K63-ubiquitinated monosomes arrested at the stop codon (Figure 3F, lane 8).

It has been suggested that the collided ribosome could act as a wedge during ASCC-mediated splitting (23), implying that if dissociation of the last ribosome in the colliding queue occurs at all, it would be inefficient. Thus, dissociation of monosomes and all (including the last) polysomal ribosomes observed in our experiments prompted us to compare the rate of dissociation of monosomes and the leading polysomal ribosomes. To follow ASCC-mediated dissociation *per se* and to exclude any influence of potential differences in ubiquitination rates, we employed SDG-purified polyubiquinated tetrasomes and monosomes. For this, polysomes were assembled in RRL on β-VHP-Stop mRNA and purified by SDG centrifugation. Ribosome-containing fractions were combined, polyubiquinated by ZNF598 and fractionated again by a second round of SDG centrifugation. Purified ubiquitinated monosomes and tetrasomes were then incubated with ASCC, and the reaction was stopped by elevation of [Mg^{2+}]. Even though release of leading ribosomes in ubiquitinated tetrasomes was faster than dissociation of monosomes, the difference was very moderate (Figure 4A, compare lanes 1–5 with lanes 6–9).

In contrast to monosomes and leading ribosomes, collided ribosomes are in pre-translocated states. In the cellular environment, collided ribosomes could be translocated by eEF2 following ASCC-mediated release of the preceding neighboring ribosome. We therefore compared the rates of dissociation of ubiquitinated tetrasomes in the presence and absence of eEF2. We did not observe any significant difference in release of either leading or collided ribosomes with and without eEF2 (Figure 4B).

To confirm that dissociation of monosomes also involves ribosomal splitting, we determined whether ASCC enables Listerin-mediated ubiquitination of NC-tRNAs in both trisomes and monosomes stalled on the polyA tract of β-VHP-A39 mRNA. Addition of Listerin and NEMF to reaction mixtures containing ZNF598 and ASCC resulted in nearly complete ubiquitination of nascent chains in trisomes and monosomes (Figure 4C, lanes 4 and 8), indicating that in both cases, ASCC efficiently split ribosomes, yielding NC-tRNA-associated 60S subunits. When the *wt* Ub was replaced by the K63R mutant, moderate ubiquitination of NCs still occurred in complexes stalled on polyA (Figure 4D, lanes 3 and 6), which is consistent with partial release of leading ribosomes in these conditions (Figure 3C, lane 5).

In conclusion, ZNF598 mediates K63-polyubiquitination of eS10 and uS10 in all stalled polysomal ribosomes irrespective of their position in the collided queue. ASCC, in turn, efficiently releases monosomal and all polysomal ribosomes as long as they are polyubiquitinated by ZNF598. In both polysomes and monosomes, ASCC splits ribosomes into 40S subunits and NC-tRNA-associated 60S subunits, enabling Listerin-mediated ubiquitination of nascent chains.

The activity of ASCC on the *in vitro* reconstituted 80S ribosomal complexes

Polysomes formed in RRL can potentially be associated with factors affecting the activity of ASCC, which warranted testing of ASCC on the *in vitro* reconstituted ribosomal complexes. Thus, pre- and post-translocated 80S elongation complexes (ECs) were assembled on β-MF-Stop mRNA (containing the β-globin 5′UTR, a Met-Phe coding region and a UAA stop codon) from purified ribosomal subunits, eIFs, $Met\text{-}tRNA_i^{Met}$, $Phe\text{-}tRNA^{Phe}$ and eEF1H in the presence/absence of eEF2, and purified by SDG centrifugation. ASCC efficiently dissociated post- (Figure 5A, lanes 3 and 7), as well as pre-translocated 80S ECs that mimic the last ribosome in the stalled queue (Figure 5B, lane 6) if they were K63-polyubiquitinated by ZNF598, indicating that dissociation did not require accessory factors.

To determine the length of the overhanging 3′-terminal region of mRNA required for dissociation, we used 80S pre-termination complexes (pre-TCs) reconstituted on β-MLLFF-Stop mRNAs containing a MLLFF coding region, a UAA stop codon and 3′UTRs of different lengths. Dissociation of pre-TCs containing 80 mRNA nts downstream from the P site was assayed by toe-printing, whereas disso-

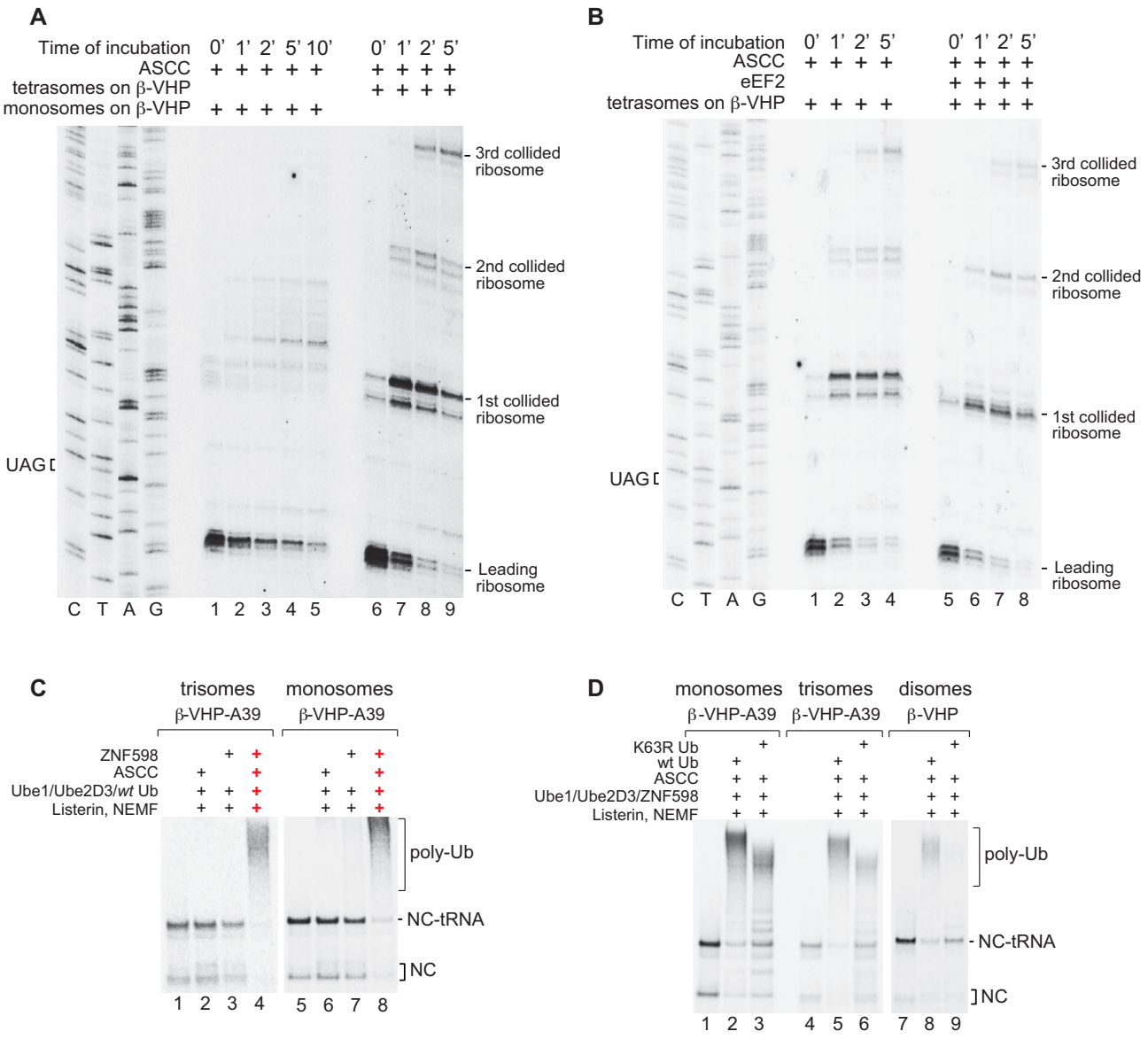

Figure 4. ASCC-mediated ribosome release in polysomes and monosomes and subsequent Listerin-mediated ubiquitination of nascent chains. (**A**) Time courses of ASCC-mediated dissociation of SDG-purified ZNF598-polyubiquitinated monosomes and tetrasomes stalled at the stop codon of β-VHP mRNA, assayed by toe-printing. (**B**) Time courses of ASCC-mediated dissociation of SDG-purified ZNF598-polyubiquitinated tetrasomes stalled at the stop codon of β-VHP mRNA in the presence/absence of eEF2, assayed by toe-printing. (**C, D**) Ubiquitination of NC-tRNAs by Listerin/NEMF following ASCC-mediated dissociation of trisomes, monosomes and disomes stalled in RRL on β-VHP-A39 and β-VHP mRNAs and ubiquitinated by ZNF598 with *wt* or K63R Ub, assayed by SDS-PAGE.

ciation of complexes containing 20 or 30 mRNA nts was monitored by SDG centrifugation. ASCC dissociated pre-TCs containing 80 or 30, but not 20 overhanging mRNA nts (Figure 5C). Ubiquitination of NCs after incubation with ZNF598/ASCC/Listerin/NEMF of disomes stalled in RRL at the stop codon of β-VHP-Stop mRNA also occurred when disomes contained 35, but not 21 or 26 overhanging 3′-terminal mRNA nts downstream from the P site (Figure 5D).

To determine the degree of K63 ubiquitination required for dissociation, we reconstituted *in vitro* polyubiquitinated and oligoubiquitinated 80S complexes on β-MF-Stop mRNA and purified them by SDG centrifugation. Polyubiquitinated complexes comprised a mixture of 80S initiation complexes (ICs) and post-translocated ECs, whereas oligo-ubiquitinated complexes were either pre- or post-translocated ECs. In oligoubiquitinated complexes, the majority of uS10 was linked to 3–5 ubiquitins and therefore contained di- and tri-Ub chains, whereas eS10 was linked to 1–5 Ub residues and therefore also contained some di- and tri-Ub chains (Figure 5E, left and center panels). Neither polyubiquitinated, nor oligoubiquitinated SDG-purified complexes contained ZNF598 (Figure 5E, right panel). ASCC alone was sufficient for dissociation of polyubiquitinated complexes, confirming that the physical presence of ZNF598 is not essential (Figure 5F). In contrast, oligo-ubiquitinated ECs were not dissociated (Figure 5G).

Thus, ASCC dissociated *in vitro* reconstituted 80S complexes irrespective of their state (pre- or post-translocated) if they contained ∼30 or more mRNA nts downstream from the P site and sufficiently long K63 Ub chains. The requirement for the number of overhanging mRNA nucleotides for disomes

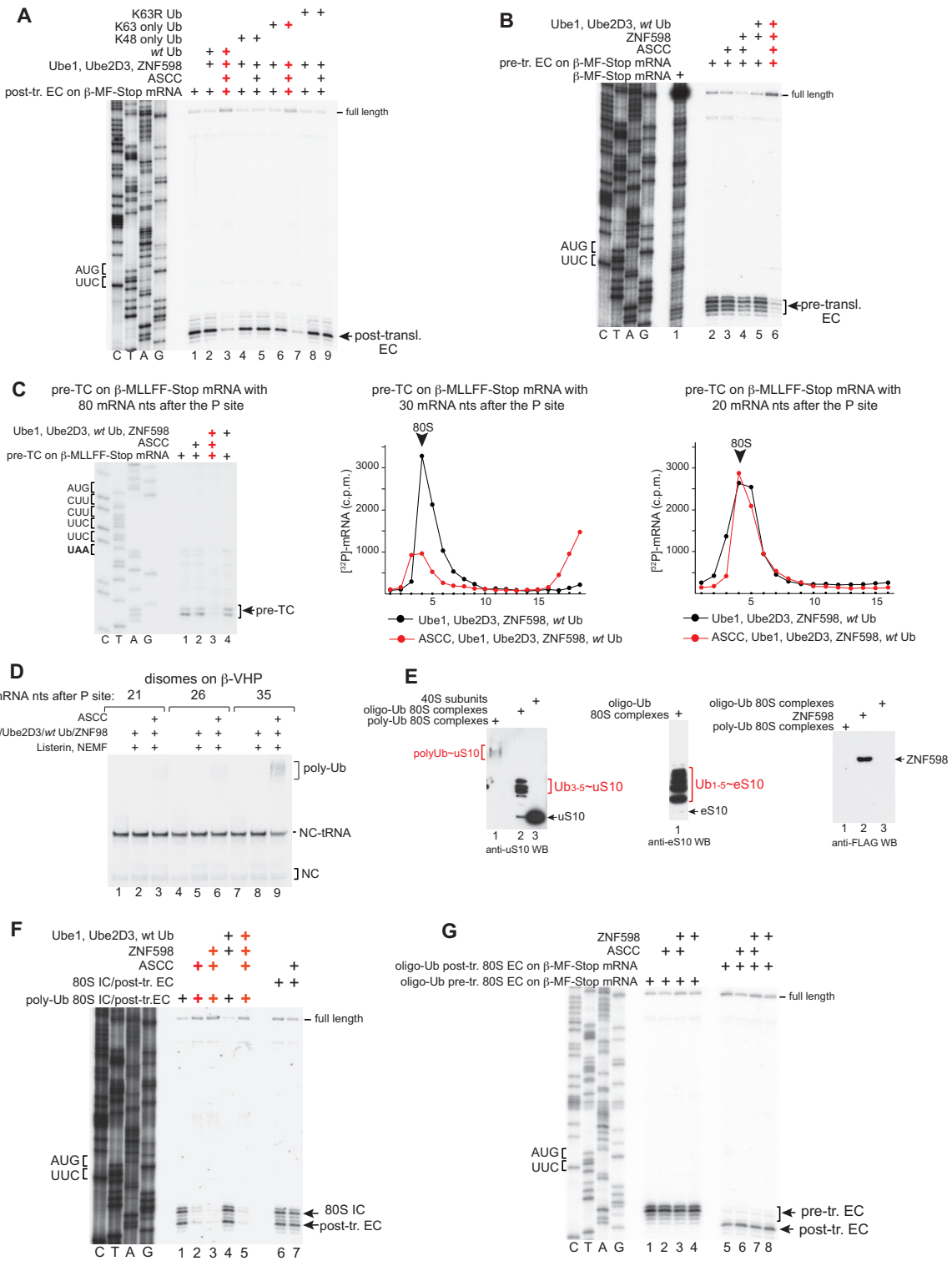

Figure 5. ASCC-mediated dissociation of *in vitro* reconstituted 80S complexes: requirements for the length of Ub chains and of the mRNA region downstream of the P site. (A, B) ASCC-mediated dissociation of (**A**) post-translocated and (**B**) pre-translocated SDG-purified 80S monosomes reconstituted *in vitro* on β-MF mRNA depending on their ubiquitination by ZNF598 with *wt*, K63 only, K48 only or K63R Ub, assayed by toe-printing. (**C**) Dependence of ASCC-mediated dissociation of ZNF598-ubiquitinated pre-TCs reconstituted *in vitro* on β-MLLFF mRNA on the length of the overhanging 3′-terminal mRNA downstream from the P site. Dissociation of complexes containing 80 overhanging mRNA nts was assayed by toe-printing (left panel), whereas dissociation of complexes containing 30 or 20 mRNA nts was assayed by SDG centrifugation (center and right panels). (**D**) Ubiquitination of NC-tRNAs by Listerin/NEMF following ASCC-mediated dissociation of disomes assembled in RRL on β-VHP mRNA and containing 21, 26 or 35 overhanging 3′-terminal mRNA nts downstream from the P site, assayed by SDS-PAGE. (**E**) The length of Ub chains and the presence of ZNF598 in SDG-purified oligoubiquitinated post-translocated 80S ECs and in a mixture of polyubiquitinated 80S ICs/post-translocated 80S ECs reconstituted *in vitro* on β-MF-Stop mRNA, assayed by western blotting using antibodies against uS10 and eS10 (left and center panels), and ZNF598 (right panel). (F, G) ASCC-mediated dissociation of (**F**) polyubiquitinated, and (**G**) oligoubiquitinated SDG-purified 80S complexes reconstituted *in vitro* on β-MF-Stop mRNA, depending on the presence of ZNF598 with/without Ube1, Ube2D3 and *wt* Ub, assayed by toe-printing.

assembled in RRL and for *in vitro* reconstituted 80S monosomes was similar.

The influence of ASCC on 48S initiation complexes

To investigate the suggested activity of ASCC in 48S complex formation (36), we employed (AUG at −6)-STEM mRNA containing a stable stem and three AUG codons: at position −6 relative to the stem, in the loop of the stem, and downstream of the stem (Figure 6A). 48S complex formation on this mRNA requires DHX29, the DExH protein that binds directly to 40S subunits and promotes initiation on structured mRNAs (46). In the absence of DHX29, 48S complexes form on the first AUG without unwinding of the stem, which becomes accommodated in the A site leading to aberrant toe-prints +11–12 nt downstream of the stem (Figure 6B, lane 2; (47)). DHX29 promotes unwinding of the stem and formation of 48S complexes with canonical +15–17 nt toe-prints from the first AUG, and also allows leaky scanning and 48S complex formation on two downstream AUGs (Figure 6B, lane 3; (47)).

ASCC alone did not substitute for DHX29 in 48S complex formation on (AUG at −6)-STEM mRNA: 48S complexes on the first AUG showed aberrant toe-prints +11–12 nt downstream of the stem, and no 48S complexes formed on downstream AUGs (Figure 6B, lane 4). Moreover, in conditions of ZNF598-mediated ubiquitination, ASCC strongly reduced 48S complex formation irrespective of whether it was added simultaneously with other translational components or after 15 minutes of incubation (Figure 6B, compare lane 2 with lanes 6 and 7). This suggested that ASCC was dissociating preformed 48S complexes. To confirm this, we employed SDG-purified 48S complexes assembled on β-MF-Stop mRNA. ASCC efficiently dissociated such complexes as long as they were K63-ubiquitinated by ZNF598 (Figure 6C, lanes 3 and 4). This activity of ASCC contrasted with the inability of the Ski complex, which contains a DExH helicase (Ski2) and disassembles 80S ribosomal complexes by extracting mRNA in the 3′→5′ direction in a nucleotide-by-nucleotide manner (48), to dissociate ribosomal complexes that did not contain 60S subunits (Figure 6D, lane 2; (48)).

The effects of RNF10-mediated ubiquitination of ribosomal protein uS3

Ribosomal protein uS3 is located at the mRNA entrance and is mono-ubiquitinated by the E3 ubiquitin ligase RNF10 (25,49,50). Regarding the reported Hel2-mediated polyubiquitination of uS3 following its mono-ubiquitination by Mag2 (25) as well as the ribosomal position of uS3, we investigated its ubiquitination by RNF10/ZNF598 and the influence of such ubiquitination on ASCC-mediated dissociation of polysomes. In vacant 80S ribosomes, recombinant RNF10 (Figure 7A) mono-ubiquitinated uS3 and formed a small amount of di-ubiquitinated product (Figure 7B, left panel, lane 4). ZNF598 was able to add several Ub moieties to RNF10-ubiquitinated uS3 yielding oligoubiquitinated protein, but it also moderately decreased the overall proportion of ubiquitinated uS3 (Figure 7B, left panel, lane 6). Polyubiquitination of uS10 and eS10 by ZNF598 was also slightly inhibited by RNF10 (Figure 7B, middle and right panels, compare lanes 2 and 6), suggesting that RNF10 and ZNF598 compete for ribosomal binding. ZNF598-mediated polyubiquitination of uS10 and eS10 in the presence of RNF10 was partially restored by EDF1 (Figure 7B, middle and right panels, compare lanes 6 and 7), a mammalian homologue of yeast Mbf1 which binds at the mRNA entrance and interacts with uS3 (51). Interestingly, we also observed low-level RNF10-induced mono-ubiquitination of uS10 and eS10 (Figure 7B, middle and right panels, lanes 4).

To assay the influence of uS3 ubiquitination on the activity of ASCC, SDG-purified tetrasomes stalled in RRL on β-VHP-Stop mRNA were first ubiquitinated by RNF10 and ZHF598 individually or in combination, then incubated with ASCC, after which ribosomal complexes were analyzed by toe-printing. ASCC efficiently dissociated polysomes ubiquitinated by ZNF598 alone or in combination with RNF10, but not those ubiquitinated by RNF10 alone (Figure 7C, lanes 3–5). Thus, ubiquitination of uS3 alone did not support the activity of ASCC, but also did not influence it when ribosomes in addition were ubiquitinated on uS10 and eS10 by ZNF598.

However, we noticed a +1–2nt toe-print shift of the leading ribosome in the presence of RNF10 (Figures 7C, lanes 4–6). In purified 80S initiation complexes formed on β-MF-Stop mRNA, RNF10 induced the shift only in the presence of the ubiquitination mixture, indicating that the shift required uS3 ubiquitination (Figure 7D). To assay the influence of the ribosomal state on this shift, we employed pre- and post-translocated collided ribosomes obtained by incubation of disomes formed on β-VHP-Stop mRNA with eRFs/ABCE1 in the absence or presence of eEF2. The RNF10-dependent shift was more pronounced in the case of the post-translocated ribosome (Figure 7E). Although it cannot be excluded that ubiquitinated pre-translocated ribosomes simply did not exhibit the shift, it is also possible that RNF10 preferentially ubiquitinated non-rotated post-translocated ribosomal complexes.

Discussion

In vitro reconstitution revealed that ASCC efficiently dissociated stalled monosomes, all ribosomes in stalled polysomes irrespective of their position in a queue, *in vitro* reconstituted 80S elongation complexes in both pre- and post-translocated states, as well as 48S initiation complexes. Dissociation strictly required ribosomal polyubiquitination by ZNF598 and occurred in complexes containing ≥ 30–35 overhanging 3′-terminal mRNA nt. downstream from the P site. However, ribosomal collision was not a prerequisite for either ribosomal ubiquitination or release. ASCC-mediated dissociation of polysomes and monosomes both involved ribosomal splitting into 40S subunits and NC-tRNA-associated 60S subunits, enabling the next step in the RQC pathway, namely nascent chain ubiquitination by Listerin.

Ribosomal ubiquitination by ZNF598

Early reports suggested that to initiate RQC in mammals, ZNF598 preferentially mono-ubiquitinates uS10 and eS10 (6,7,10). However, a more recent report showed that like its yeast homologue Hel2, ZNF598 functionally K63-polyubiquitinates uS10 in collided mammalian ribosomes, priming them for disassembly by ASCC (22). In agreement with this report, we also found that ZNF598 mediates K63-specific polyubiquitination of uS10, and in addition, observed equally strong polyubiquitination of eS10. However, in contrast to previous reports (e.g. (8)), we found that ribosomal collision was not a prerequisite for ribosomal ubiquitination,

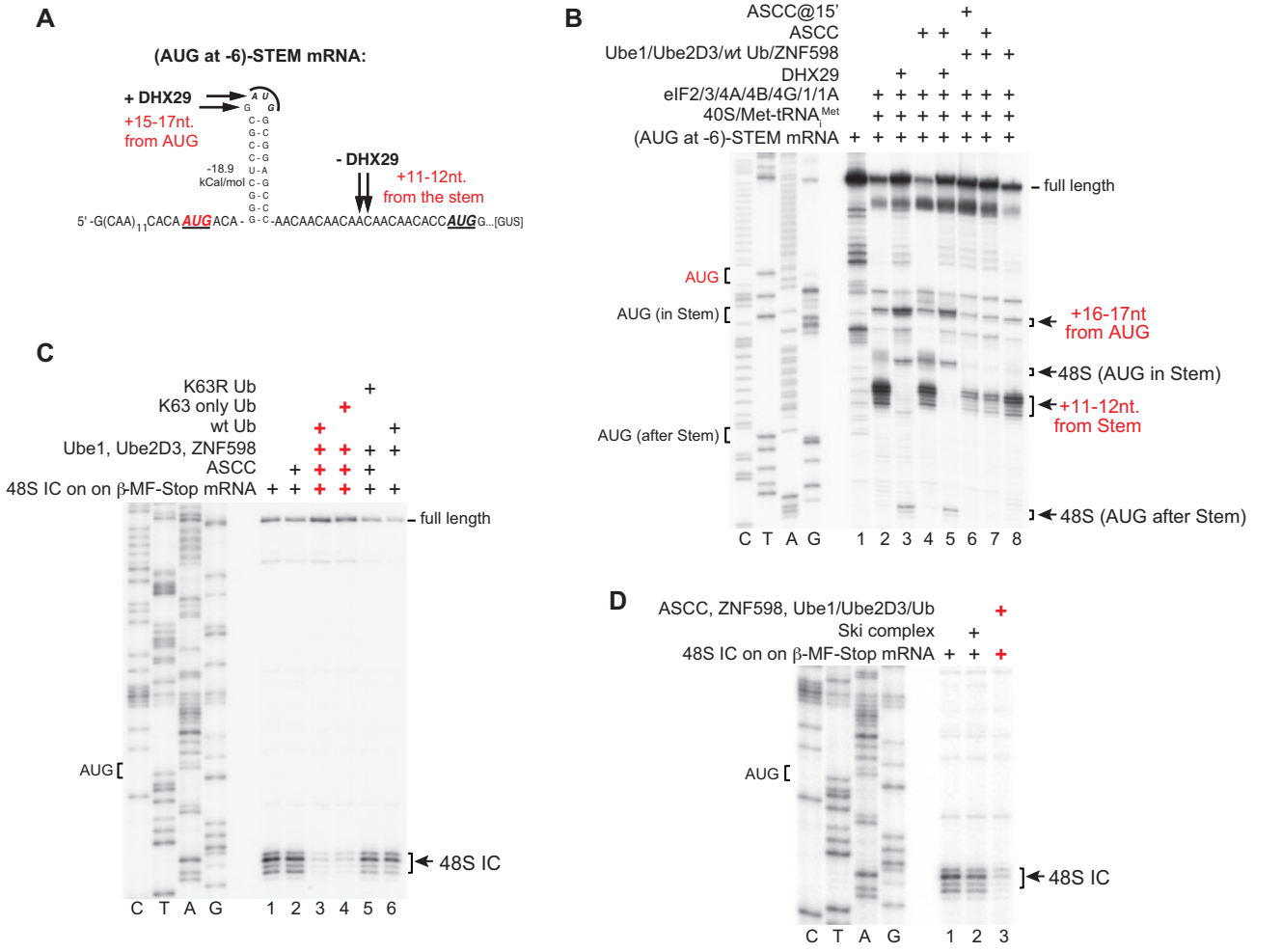

Figure 6. ASCC-mediated dissociation of 48S initiation complexes. (**A**) Sequence of the 5′ UTR of (AUG at −6)-STEM mRNA, containing three AUG triplets: 6 nt before the stem, in the loop of the stem, and 21 nt downstream from the stem: positions of toe-prints of 48S complexes assembled with/without DHX29 are indicated by arrows. (**B**) The influence of ASCC and ZNF598/Ube1/Ube2D3/Ub on 48S complex formation on (AUG at −6)-STEM mRNA in the presence/absence of DHX29 and indicated translation components, assayed by toe-printing. (**C, D**) Dissociation by ASCC or by the Ski complex of SDG-purified 48S ICs reconstituted *in vitro* on β-MF mRNA by ASCC depending on their ubiquitination by ZNF598 with *wt*, K63 only or K63R Ub, assayed by toe-printing.

and that ZNF598 can efficiently K63-polyubiquitinate uS10 and eS10 in stalled polysomes, 80S monosomes, vacant 80S ribosomes, and individual 40S subunits.

This promiscuous ability of ZNF598 to ubiquitinate a variety of ribosomal complexes can be restricted by *trans*-acting factors, as exemplified by the inhibition of ubiquitination of vacant 80S ribosomes by SERBP1 alone and in combination with eEF2. Such inhibition would spare translationally inactive ribosomes associated with SERBP1/eEF2 from futile cycles of ubiquitination and deubiquitination. Although the exact ribosomal position of ZNF598/Hel2 has not been determined, cross-linking studies placed Hel2 in close proximity to eS3, eS10 and uS10 (52), and binding of SERBP1 and its yeast homolog Stm1 to eS10 (41) may therefore impair binding of ZNF598 to the 40S subunit or prevent it from gaining access to target residues in eS10 and adjacent ribosomal proteins. It remains to be determined whether other proteins that sequester ribosomes in an inactive state (e.g. (41,53,54)) protect them from regulatory ubiquitination as well.

ZNF598 also promoted robust synthesis of free K63-linked polyubiquitin chains in the absence of ribosomal substrates. This indicates that ZNF598 must contain a site for efficient binding of acceptor ubiquitin that orients it such that K63 is positioned to attack the E2-Ub conjugate. The functional importance of this activity is not known, but unanchored ubiquitin chains are involved in diverse processes, including stress and innate immune responses (55–57). Synthesis of polyubiquitin chains with K63 linkage in the absence of a substrate was also reported for RNF216, a RING-between-RING E3 ligase, in which case the acceptor ubiquitin binds to a composite surface formed by the C-terminal region of the RING2 domain and its zinc finger insertion (58). The N-terminal RING domain of ZNF598 is followed by five predicted C_2H_2-type zinc finger motifs, the first four of which are conserved between ZNF598 and Hel2, whereas the region containing the C-terminal zinc finger motif is not essential for ZNF598 function (6). One or more of the four N-terminal zinc finger motifs of ZNF598 could be involved in an interaction with the acceptor ubiquitin. Our observation that ZNF598 can catalyze formation of di- but not longer Ub chains with non-K63 linkages (Figure 1E) could potentially reflect its higher affinity to di- (or tri-) Ub chains than to single Ub moieties that would

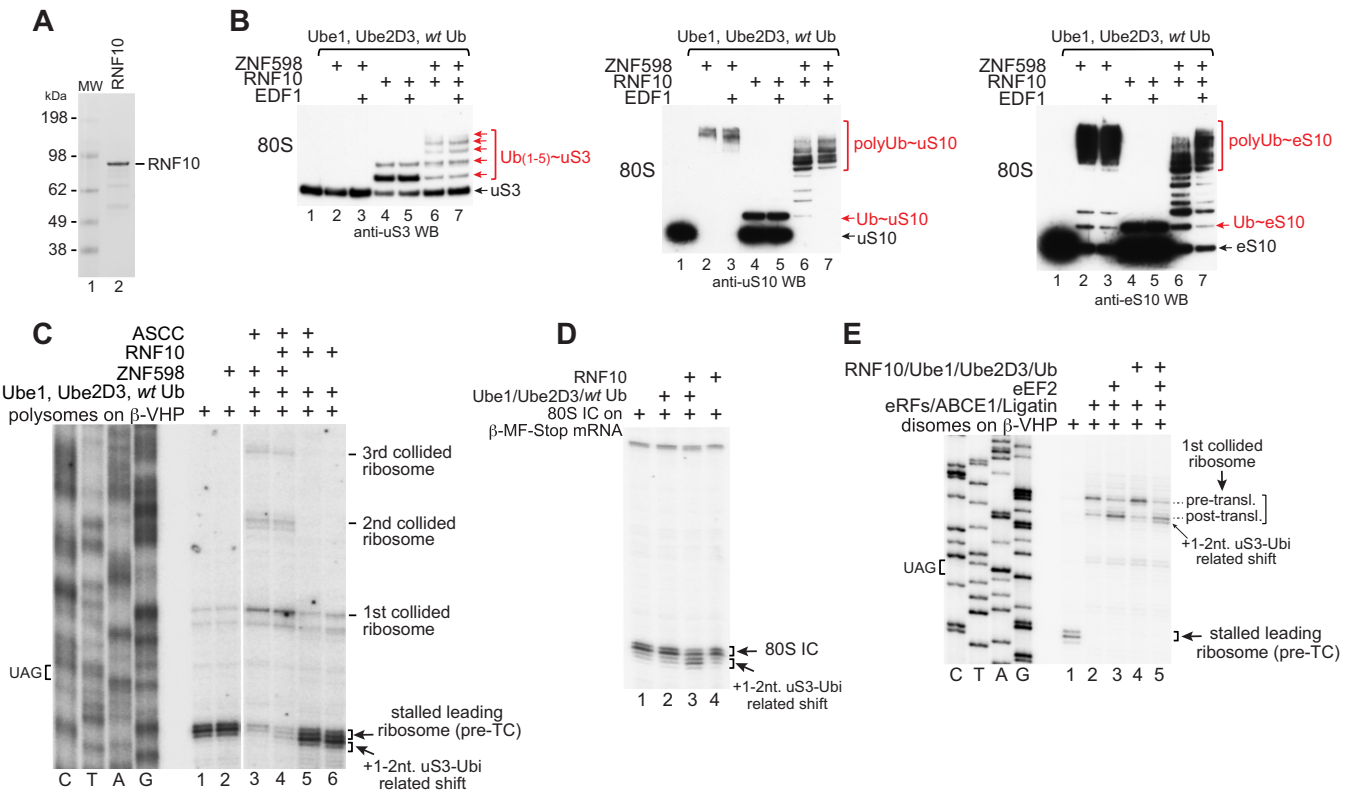

Figure 7. Ribosomal ubiquitination by RNF10. (**A**) Purified RNF10, analyzed by SDS-PAGE and SimplyBlue staining. (**B**) Ubiquitination of uS3, uS10 and eS10 in vacant 80S ribosomes by ZNF598 and/or RNF10 with Ube1, Ube2D3 and *wt* Ub in the presence/absence of EDF1, assayed by western blotting using antibodies against ribosomal proteins. (**C**) ASCC-mediated dissociation of SDG-purified heavy polysomes stalled in RRL at the stop codon of β-VHP mRNA depending on their ubiquitination by ZNF598 and/or RNF10, assayed by toe-printing. Separation of two parts of the gel by the white line indicates that the juxtaposed parts were from the same gel. (D, E) Characterization of the RNF10-induced +1–2nt toe-print shift, using (**D**) 80S ICs reconstituted *in vitro* on β-MF mRNA, and (**E**) collided ribosomes in pre- and post-translocated states obtained by incubation of disomes formed on β-VHP mRNA in RRL with eRFs/ABCE1/Ligatin in the presence/absence of eEF2.

result in higher probability of the specific orientation of the acceptor ubiquitin in Ub chains.

ASCC-mediated dissociation of ribosomal complexes

Contrary to previous reports (14,22,31), we found that in stalled polysomes, ASCC released all ribosomes, including the last collided one. ASCC also efficiently dissociated 80S monosomes assembled in RRL or reconstituted *in vitro*. The fact that incubation of monosomes with ZNF598 and ASCC rendered nascent chains susceptible to ubiquitination by Listerin confirmed that ASCC induced *bona fide* ribosomal splitting. Susceptibility to dissociation is thus not limited by the occurrence of collision or the position of ribosomes in polysomal queues. Moreover, contrary to the reported stimulation of initiation by scanning ribosomal complexes on a subset of cellular mRNAs containing stable secondary structures (36), we observed efficient dissociation of 48S initiation complexes by ASCC.

Consistent with the reported activity of RQT (23), we found that ASCC-mediated ribosomal splitting also depends on an overhanging 3′-terminal region of mRNA. The identified requirements of ≥30–35 overhanging 3′-terminal mRNA nt. downstream from the P site for the ASCC function is in direct contrast to the requirements of the Ski complex, which could extract mRNA from complexes containing as few as 16 nt. downstream of the P site (48). This difference reflects the distinct ribosomal positions and orientations of Ski2 and Slh1/ASCC3 helicase domains. Thus, whereas the single Ski2 helicase domain is positioned and oriented to directly accept mRNA protruding from the entry site of the 40S subunit (59), the N-terminal helicase domain of Slh1, although also positioned at the mRNA entrance, is inappropriately oriented to accept the protruding mRNA directly, whereas its C-terminal helicase cassette is oriented such that it could bind mRNA and extract it from the 40S subunit but resides at some distance from the mRNA entry site (23). In the structure of ribosome-bound Slh1 (23), a 30–35nt extension of mRNA from the P site should be sufficient for engagement with the C-terminal cassette. The model for RQT/ASCC function suggests that the force imposed during mRNA extraction from the stalled ribosome exploits the adjacent collided ribosome as a wedge to mediate dissociation (23). We found that ASCC-mediated dissociation of monosomal ribosomes was somewhat slower than dissociation of the leading polysomal ribosomes, which could reflect the proposed role of collided ribosomes in the mechanism of dissociation. However, dissociation of 80S monosomes reported here was nevertheless very efficient, which indicates that the suggested role for the collided ribosome is not essential for dissociation.

Although our data confirmed the previously reported absolute dependence of ASCC function on ZNF598-mediated ubiquitination and general requirements for long Ub chains

(14,22), the level of ubiquitination sufficient for ribosomal release varied depending on the nature of stalling. Thus, ASCC induced moderate dissociation of monosomes and polysomes stalled on a polyA tract after their ubiquitination with K63R Ub, in which case ZNF598 can synthesize only di-Ub chains with non-K63 linkage. Although the basis for the observed dissociation of ribosomes stalled on a polyA tract is obscure, it is worth noting that in leading ribosomes stalled on polyA, adenosines in the A site adopt a single-stranded helical, decoding-incompetent conformation (24,43), and that a large proportion of the first collided ribosomes are in post- rather than in pre-translocated states (24). Such structural changes could potentially influence susceptibility to dissociation by ASCC. The polyA tract downstream of the P site was also sufficiently long to interact with ASCC3, and if ASCC3 has specific affinity to polyA, it could also aid ribosomal association of ASCC when Ub chains are very short.

Our finding that collision is not required for ribosomal ubiquitination and release raises the question of how and whether these activities are regulated. Association with SERBP1 and eEF2 would spare transitionally inactive 80S ribosomes from ubiquitination. The ability of ZNF598 to ubiquitinate actively translating ribosomes is not known, and it could be substantially lower than for stalled polysomes. However, even if an actively translating ribosome is ubiquitinated, it is unlikely that it will be dissociated because ASCC depends on interaction with the 3′-overhanging region of mRNA, but kinetically, ASCC-mediated dissociation is ∼40x slower than each elongation cycle (60,61). The cytoplasmic abundance of ASCC subunits is much lower than that of ZNF598, and both are much less abundant than ribosomes (https://pax-db.org/), so that a delay between ubiquitination and recruitment of ASCC is feasible. Since ubiquitination of ribosomal proteins is dynamic and is reversed by specific deubiquitinases (62–64) that have been reported to associate with polysomes (64), the ubiquitination and thus the susceptibility of ribosomes to ASCC-mediated dissociation are also potentially regulatable in this way.

Data availability

The data underlying this article are available in the article and in its online supplementary material.

Supplementary data

Supplementary Data are available at NAR Online.

Acknowledgements

We dedicate this work to the memory of our friend and colleague Alexander Bulakhov, who was one of the motive forces in the design and conduct of experiments, analysis of data and writing of the manuscript. Alexander was tragically killed defending his wife and daughter during an armed robbery. This occurred during the final stages of manuscript preparation, and he was therefore not able to approve the final accepted version.

We thank Rustam Ayupov for purification of the Ski complex and Andrew Tcherepanov for expert technical assistance.

Funding

National Institutes of Health [R35 GM122602 to T.P., R01 GM097014 to C.H.]. Funding for open access charge: NIH [R35 GM122602].

Conflict of interest statement

None declared.

References

1. D'Orazio,K.N. and Green,R. (2021) Ribosome states signal RNA quality control. *Mol. Cell*, **81**, 1372–1383.
2. Yip,M.C.J. and Shao,S. (2021) Detecting and rescuing stalled ribosomes. *Trends Biochem. Sci.*, **46**, 731–743.
3. Matsuo,Y. and Inada,T. (2023) Co-translational quality control induced by translational arrest. *Biomolecules*, **13**, 317.
4. Sitron,C.S. and Brandman,O. (2020) Detection and degradation of stalled nascent chains via ribosome-associated quality control. *Annu. Rev. Biochem.*, **89**, 417–442.
5. Filbeck,S., Cerullo,F., Pfeffer,S. and Joazeiro,C.A.P. (2022) Ribosome-associated quality-control mechanisms from bacteria to humans. *Mol. Cell*, **82**, 1451–1466.
6. Garzia,A., Jafarnejad,S.M., Meyer,C., Chapat,C., Gogakos,T., Morozov,P., Amiri,M., Shapiro,M., Molina,H., Tuschl,T., *et al.* (2017) The E3 ubiquitin ligase and RNA-binding protein ZNF598 orchestrates ribosome quality control of premature polyadenylated mRNAs. *Nat. Commun.*, **8**, 16056.
7. Juszkiewicz,S. and Hegde,R.S. (2017) Initiation of quality control during poly(A) translation requires site-specific ribosome ubiquitination. *Mol. Cell*, **65**, 743–750.
8. Juszkiewicz,S., Chandrasekaran,V., Lin,Z., Kraatz,S., Ramakrishnan,V. and Hegde,R.S. (2018) ZNF598 Is a quality control sensor of collided ribosomes. *Mol. Cell*, **72**, 469–481.
9. Matsuo,Y., Ikeuchi,K., Saeki,Y., Iwasaki,S., Schmidt,C., Udagawa,T., Sato,F., Tsuchiya,H., Becker,T., Tanaka,K., *et al.* (2017) Ubiquitination of stalled ribosome triggers ribosome-associated quality control. *Nat. Commun.*, **8**, 159.
10. Sundaramoorthy,E., Leonard,M., Mak,R., Liao,J., Fulzele,A. and Bennett,E.J. (2017) ZNF598 and RACK1 regulate mammalian ribosome-associated quality control function by mediating regulatory 40S ribosomal ubiquitylation. *Mol. Cell*, **65**, 751–760.
11. Ikeuchi,K., Tesina,P., Matsuo,Y., Sugiyama,T., Cheng,J., Saeki,Y., Tanaka,K., Becker,T., Beckmann,R. and Inada,T. (2019) Collided ribosomes form a unique structural interface to induce Hel2-driven quality control pathways. *EMBO J.*, **38**, e100276.
12. Sitron,C.S., Park,J.H. and Brandman,O. (2017) Asc1, Hel2, and Slh1 couple translation arrest to nascent chain degradation. *RNA*, **23**, 798–810.
13. Hashimoto,S., Sugiyama,T., Yamazaki,R., Nobuta,R. and Inada,T. (2020) Identification of a novel trigger complex that facilitates ribosome-associated quality control in mammalian cells. *Sci. Rep.*, **10**, 3422.
14. Juszkiewicz,S., Speldewinde,S.H., Wan,L., Svejstrup,J.Q. and Hegde,R.S. (2020) The ASC-1 complex disassembles collided ribosomes. *Mol. Cell*, **79**, 603–614.
15. Defenouillère,Q., Yao,Y., Mouaikel,J., Namane,A., Galopier,A., Decourty,L., Doyen,A., Malabat,C., Saveanu,C., Jacquier,A., *et al.* (2013) Cdc48-associated complex bound to 60S particles is required for the clearance of aberrant translation products. *Proc. Natl. Acad. Sci. U.S.A.*, **110**, 5046–5051.
16. Lyumkis,D., Oliveira dos Passos,D., Tahara,E.B., Webb,K., Bennett,E.J., Vinterbo,S., Potter,C.S., Carragher,B. and Joazeiro,C.A. (2014) Structural basis for translational surveillance by the large ribosomal subunit-associated protein quality control complex. *Proc. Natl. Acad. Sci. U.S.A.*, **111**, 15981–15986.

17. Shao,S., Brown,A., Santhanam,B. and Hegde,R.S. (2015) Structure and assembly pathway of the ribosome quality control complex. *Mol. Cell*, **57**, 433–444.
18. Kuroha,K., Zinoviev,A., Hellen,C.U.T. and Pestova,T.V. (2018) Release of ubiquitinated and non-ubiquitinated nascent chains from stalled mammalian ribosomal complexes by ANKZF1 and Ptrh1. *Mol. Cell*, **72**, 286–302.
19. Verma,R., Reichermeier,K.M., Burroughs,A.M., Oania,R.S., Reitsma,J.M., Aravind,L. and Deshaies,R.J. (2018) Vms1 and ANKZF1 peptidyl-tRNA hydrolases release nascent chains from stalled ribosomes. *Nature*, **557**, 446–451.
20. Zurita Rendón,O., Fredrickson,E.K., Howard,C.J., Van Vranken,J., Fogarty,S., Tolley,N.D., Kalia,R., Osuna,B.A., Shen,P.S., Hill,C.P., *et al.* (2018) Vms1p is a release factor for the ribosome-associated quality control complex. *Nat. Commun.*, **9**, 2197.
21. Yip,M.C.J., Keszei,A.F.A., Feng,Q., Chu,V., McKenna,M.J. and Shao,S. (2019) Mechanism for recycling tRNAs on stalled ribosomes. *Nat. Struct. Mol. Biol.*, **26**, 343–349.
22. Narita,M., Denk,T., Matsuo,Y., Sugiyama,T., Kikuguchi,C., Ito,S., Sato,N., Suzuki,T., Hashimoto,S., Machová,I., *et al.* (2022) A distinct mammalian disome collision interface harbors K63-linked polyubiquitination of uS10 to trigger hRQT-mediated subunit dissociation. *Nat. Commun.*, **13**, 6411.
23. Best,K., Ikeuchi,K., Kater,L., Best,D., Musial,J., Matsuo,Y., Berninghausen,O., Becker,T., Inada,T. and Beckmann,R. (2023) Structural basis for clearing of ribosome collisions by the RQT complex. *Nat. Commun.*, **14**, 921.
24. Tesina,P., Lessen,L.N., Buschauer,R., Cheng,J., Wu,C.C., Berninghausen,O., Buskirk,A.R., Becker,T., Beckmann,R. and Green,R. (2020) Molecular mechanism of translational stalling by inhibitory codon combinations and poly(A) tracts. *EMBO J.*, **39**, e103365.
25. Sugiyama,T., Li,S., Kato,M., Ikeuchi,K., Ichimura,A., Matsuo,Y. and Inada,T. (2019) Sequential ubiquitination of ribosomal protein uS3 triggers the degradation of non-functional 18S rRNA. *Cell Rep.*, **26**, 3400–3415.
26. Jung,D.J., Sung,H.S., Goo,Y.W., Lee,H.M., Park,O.K., Jung,S.Y., Lim,J., Kim,H.J., Lee,S.K., Kim,T.S., *et al.* (2002) Novel transcription coactivator complex containing activating signal cointegrator 1. *Mol. Cell. Biol.*, **22**, 5203–5211.
27. Soll,J.M., Brickner,J.R., Mudge,M.C. and Mosammaparast,N. (2018) RNA ligase-like domain in activating signal cointegrator 1 complex subunit 1 (ASCC1) regulates ASCC complex function during alkylation damage. *J. Biol. Chem.*, **293**, 13524–13533.
28. Stoneley,M., Harvey,R.F., Mulroney,T.E., Mordue,R., Jukes-Jones,R., Cain,K., Lilley,K.S., Sawarkar,R. and Willis,A.E. (2022) Unresolved stalled ribosome complexes restrict cell-cycle progression after genotoxic stress. *Mol. Cell*, **82**, 1557–1572.
29. Dango,S., Mosammaparast,N., Sowa,M.E., Xiong,L.J., Wu,F., Park,K., Rubin,M., Gygi,S., Harper,J.W. and Shi,Y. (2011) DNA unwinding by ASCC3 helicase is coupled to ALKBH3-dependent DNA alkylation repair and cancer cell proliferation. *Mol. Cell*, **44**, 373–384.
30. Jia,J., Absmeier,E., Holton,N., Pietrzyk-Brzezinska,A.J., Hackert,P., Bohnsack,K.E., Bohnsack,M.T. and Wahl,M.C. (2020) The interaction of DNA repair factors ASCC2 and ASCC3 is affected by somatic cancer mutations. *Nat. Commun.*, **11**, 5535.
31. Matsuo,Y., Tesina,P., Nakajima,S., Mizuno,M., Endo,A., Buschauer,R., Cheng,J., Shounai,O., Ikeuchi,K., Saeki,Y., *et al.* (2020) RQT complex dissociates ribosomes collided on endogenous RQC substrate SDD1. *Nat. Struct. Mol. Biol.*, **27**, 323–332.
32. Shih,S.C., Prag,G., Francis,S.A., Sutanto,M.A., Hurley,J.H. and Hicke,L.(2003) A ubiquitin-binding motif required for intramolecular monoubiquitylation, the CUE domain. *EMBO J.*, **22**, 1273–1281.
33. Lombardi,P.M., Haile,S., Rusanov,T., Rodell,R., Anoh,R., Baer,J.G., Burke,K.A., Gray,L.N., Hacker,A.R., Kebreau,K.R., *et al.* (2022) The ASCC2 CUE domain in the ALKBH3-ASCC DNA repair complex recognizes adjacent ubiquitins in K63-linked polyubiquitin. *J. Biol. Chem.*, **298**, 101545.
34. Matsuo,Y., Uchihashi,T. and Inada,T. (2023) Decoding of the ubiquitin code for clearance of colliding ribosomes by the RQT complex. *Nat. Commun.*, **14**, 79.
35. Flis,J., Holm,M., Rundlet,E.J., Loerke,J., Hilal,T., Dabrowski,M., Bürger,J., Mielke,T., Blanchard,S.C., Spahn,C.M.T., *et al.* (2018) tRNA translocation by the eukaryotic 80S ribosome and the impact of GTP hydrolysis. *Cell Rep.*, **25**, 2676–2688.
36. Kito,Y., Matsumoto,A., Ichihara,K., Shiraishi,C., Tang,R., Hatano,A., Matsumoto,M., Han,P., Iwasaki,S. and Nakayama,K.I. (2023) The ASC-1 complex promotes translation initiation by scanning ribosomes. *EMBO J.*, **24**, e112869.
37. Pisarev,A.V., Unbehaun,A., Hellen,C.U. and Pestova,T.V. (2007) Assembly and analysis of eukaryotic translation initiation complexes. *Methods Enzymol.*, **430**, 147–177.
38. Saito,K., Horikawa,W. and Ito,K. (2015) Inhibiting K63 polyubiquitination abolishes no-go type stalled translation surveillance in *Saccharomyces cerevisiae*. *PLoS Genet.*, **11**, e1005197.
39. Anger,A.M., Armache,J.P., Berninghausen,O., Habeck,M., Subklewe,M., Wilson,D.N. and Beckmann,R. (2013) Structures of the human and Drosophila 80S ribosome. *Nature*, **497**, 80–85.
40. Zinoviev,A., Hellen,C.U.T. and Pestova,T.V. (2015) Multiple mechanisms of reinitiation on bicistronic calicivirus mRNAs. *Mol. Cell*, **57**, 1059–1073.
41. Brown,A., Baird,M.R., Yip,M.C., Murray,J. and Shao,S. (2018) Structures of translationally inactive mammalian ribosomes. *eLife*, **7**, e40486.
42. Shao,S., von der Malsburg,K. and Hegde,R.S. (2013) Listerin-dependent nascent protein ubiquitination relies on ribosome subunit dissociation. *Mol. Cell*, **50**, 637–648.
43. Chandrasekaran,V., Juszkiewicz,S., Choi,J., Puglisi,J.D., Brown,A., Shao,S., Ramakrishnan,V. and Hegde,R.S. (2019) Mechanism of ribosome stalling during translation of a poly(A) tail. *Nat. Struct. Mol. Biol.*, **26**, 1132–1140.
44. Arthur,L., Pavlovic-Djuranovic,S., Smith-Koutmou,K., Green,R., Szczesny,P. and Djuranovic,S. (2015) Translational control by lysine-encoding A-rich sequences. *Sci. Adv.*, **1**, e1500154.
45. Alkalaeva,E.Z., Pisarev,A.V., Frolova,L.Y., Kisselev,L.L. and Pestova,T.V. (2006) In vitro reconstitution of eukaryotic translation reveals cooperativity between release factors eRF1 and eRF3. *Cell*, **125**, 1125–1136.
46. Pisareva,V.P., Pisarev,A.V., Komar,A.A., Hellen,C.U. and Pestova,T.V. (2008) Translation initiation on mammalian mRNAs with structured 5'UTRs requires DExH-box protein DHX29. *Cell*, **135**, 1237–1250.
47. Abaeva,I.S., Marintchev,A., Pisareva,V.P., Hellen,C.U. and Pestova,T.V. (2011) Bypassing of stems versus linear base-by-base inspection of mammalian mRNAs during ribosomal scanning. *EMBO J.*, **30**, 115–129.
48. Zinoviev,A., Ayupov,R.K., Abaeva,I.S., Hellen,C.U.T. and Pestova,T.V. (2020) Extraction of mRNA from stalled ribosomes by the Ski complex. *Mol. Cell*, **77**, 1340–1349.
49. Garshott,D.M., An,H., Sundaramoorthy,E., Leonard,M., Vicary,A., Harper,J.W. and Bennett,E.J. (2021) iRQC, a surveillance pathway for 40S ribosomal quality control during mRNA translation initiation. *Cell Rep.*, **36**, 109642.
50. Garzia,A., Meyer,C. and Tuschl,T. (2021) The E3 ubiquitin ligase RNF10 modifies 40S ribosomal subunits of ribosomes compromised in translation. *Cell Rep.*, **36**, 109468.
51. Sinha,N.K., Ordureau,A., Best,K., Saba,J.A., Zinshteyn,B., Sundaramoorthy,E., Fulzele,A., Garshott,D.M., Denk,T., Thoms,M., *et al.* (2020) EDF1 coordinates cellular responses to ribosome collisions. *eLife*, **9**, e58828.
52. Winz,M.L., Peil,L., Turowski,T.W., Rappsilber,J. and Tollervey,D. (2019) Molecular interactions between Hel2 and RNA supporting ribosome-associated quality control. *Nat. Commun.*, **10**, 563.

53. Wang,Y.J., Vaidyanathan,P.P., Rojas-Duran,M.F., Udeshi,N.D., Bartoli,K.M., Carr,S.A. and Gilbert,W.V. (2018) Lso2 is a conserved ribosome-bound protein required for translational recovery in yeast. *PLoS Biol.*, **16**, e2005903.
54. Wells,J.N., Buschauer,R., Mackens-Kiani,T., Best,K., Kratzat,H., Berninghausen,O., Becker,T., Gilbert,W., Cheng,J. and Beckmann,R. (2020) Structure and function of yeast Lso2 and human CCDC124 bound to hibernating ribosomes. *PLoS Biol.*, **18**, e3000780.
55. Blount,J.R., Johnson,S.L. and Todi,S.V. (2020) Unanchored ubiquitin chains, revisited. Front. *Cell. Dev. Biol.*, **8**, 582361.
56. Liu,P., Gan,W., Su,S., Hauenstein,A.V., Fu,T.M., Brasher,B., Schwerdtfeger,C., Liang,A.C., Xu,M. and Wei,W. (2018) K63-linked polyubiquitin chains bind to DNA to facilitate DNA damage repair. *Sci. Signal.*, **11**, eaar8133.
57. Song,B., Chen,Y., Liu,X., Yuan,F., Tan,E.Y.J., Lei,Y., Song,N., Han,Y., Pascal,B.D., Griffin,P.R., *et al.* (2021) Ordered assembly of the cytosolic RNA-sensing MDA5-MAVS signaling complex via binding to unanchored K63-linked poly-ubiquitin chains. *Immunity*, **54**, 2218–2230.
58. Cotton,T.R., Cobbold,S.A., Bernardini,J.P., Richardson,L.W., Wang,X.S. and Lechtenberg,B.C. (2022) Structural basis of K63-ubiquitin chain formation by the Gordon-Holmes syndrome RBR E3 ubiquitin ligase RNF216. *Mol. Cell*, **82**, 598–615.
59. Schmidt,C., Kowalinski,E., Shanmuganathan,V., Defenouillère,Q., Braunger,K., Heuer,A., Pech,M., Namane,A., Berninghausen,O., Fromont-Racine,M., *et al.* (2016) The cryo-EM structure of a ribosome-Ski2-Ski3-Ski8 helicase complex. *Science*, **354**, 1431–1433.
60. Ingolia,N.T., Lareau,L.F. and Weissman,J.S. (2011) Ribosome profiling of mouse embryonic stem cells reveals the complexity and dynamics of mammalian proteomes. *Cell*, **147**, 789–802.
61. Livingston,N.M., Kwon,J., Valera,O., Saba,J.A., Sinha,N.K., Reddy,P., Nelson,B., Wolfe,C., Ha,T., Green,R., *et al.* (2023) Bursting translation on single mRNAs in live cells. *Mol. Cell*, **83**, 2276–2289.
62. Meyer,C., Garzia,A., Morozov,P., Molina,H. and Tuschl,T. (2020) The G3BP1-Family-USP10 deubiquitinase complex rescues ubiquitinated 40S subunits of ribosomes stalled in translation from lysosomal degradation. *Mol. Cell*, **77**, 1193–1205.
63. Garshott,D.M., Sundaramoorthy,E., Leonard,M. and Bennett,E.J. (2020) Distinct regulatory ribosomal ubiquitylation events are reversible and hierarchically organized. *eLife*, **9**, e54023.
64. Snaurova,R., Vdovin,A., Durech,M., Nezval,J., Zihala,D., Jelinek,T., Hajek,R. and Simicek,M. (2022) Deubiquitinase OTUD1 resolves stalled translation on polyA and rare codon rich mRNAs. *Mol. Cell. Biol.*, **29**, e0026522.

Received: December 1, 2023. **Revised:** January 12, 2024. **Editorial Decision:** January 15, 2024. **Accepted:** January 29, 2024